Continuous Tensor Network States

Teresa Dimitra Karanikolaou

Munich 2020

Continuous Tensor Network States

Teresa Dimitra Karanikolaou

Master's Thesis
Ludwig–Maximilians–Universität and Technische Universität München

Munich, 23/01/2020

Supervisor: Prof. Dr. I. Cirac
Advisor: Dr. A. Tilloy

Contents

Abstract **ix**

Introduction **1**

1 Theoretical Background **5**
1.1 Tensor Network States 5
1.1.1 Matrix Product States (MPS) 6
1.1.2 Area Law 9
1.1.3 Projected Entangled Pairs State (PEPS) 11
1.2 Continuous Matrix Product States (cMPS) 12
1.2.1 Correlation functions and expectation values 13
1.2.2 Link with discrete MPS 14
1.2.3 Application on the Lieb-Liniger Model 15
1.3 Continuous Tensor Networks States (cTNS) 16
1.3.1 Correlation functions and expectation values 18
1.3.2 Restriction to Gaussian cTNS (GCTNS) 19

2 Algorithm and Analytic Computations **21**
2.1 Algorithm 21
2.2 Correlation functions for GCTNS 22
2.2.1 Closed form of the correlation functions 24
2.3 Computation of derivatives 25
2.3.1 Derivatives of correlation functions 25
2.3.2 Derivatives of the norm 27

3 Applications and results **31**
3.1 A simple model: Exact solution 31
3.2 Understanding the motivation for the model 31
3.3 Exact Solution 33
3.4 GCTNS in 1d 36
3.4.1 Comparison of correlation functions 42
3.5 GCTNS in 2 dimensions 42
3.5.1 Divergent terms of the GCTNS 43

3.5.2 Variational Method on non-divergent terms 45

Discussion **49**

Appendices **51**

A Appendix: Tensor Network Notation **53**
A.1 Singular Value Decomposition (SVD) 54
A.2 Tensor Networks 55

B Appendix: Path integral formulation **59**

C Appendix: Integrals **61**
C.1 One dimension 61
C.2 Two dimensions 62

Acknowledgments

I would like to express my sincere gratitude to my thesis supervisor Pr. Dr. Cirac. Moreover, I would like to thank my advisor Dr. Antoine Tilloy for his guidance, keen interest and encouragement while developing this project. His support has been invaluable. I am also grateful for the helpful discussions with colleagues from the MPQ group, especially Patrick Emonts, Tommaso Guaita and Clemént Delcamp. I take this opportunity to especially thank my friends and master colleagues Jasper van der Kolk, Michael Zantedeschi and Juan Sebastian Valbuena Bermudez for their emotional support and remarkable suggestions. I am very grateful to DAAD, as it provided me the financial support needed to complete my master's program. Finally I would like to thank my family and friends who were a constant source of motivation during my years of study

Abstract

The physical understanding of quantum many-body systems is hindered by the fact that the number of parameters describing the physical state grows exponentially with the number of degrees of freedom. Consequently, it is notoriously hard to solve strongly coupled Quantum field theories as they have infinitely many degrees of freedom. A new variational class of states aimed at dealing with strongly coupled QFT was recently put forward in [Physical Review X 9 (2), 021040]. This class is obtained as the continuum limit of Tensor Network States, which have been extremely successful on the lattice, both theoretically and numerically. However, the success of this continuum ansatz has so far not been demonstrated. In this report, a subclass of continuous Tensor Network States, the gaussian continuous Tensor Network states, are tested on a simple quasifree bosonic Hamiltonian, in one and two spacial dimensions. The variational algorithm performs succesfully in both cases. Particularly, in the two dimensional case the implementation is not trivial, due to the appearance of infinities in the energy density.

Introduction

It has always been a big challenge to describe many body quantum physics, especially in cases where the interactions between the particles are strong or long ranged. The main difficulty arises from the fact that the Hilbert space describing the many-body state, is growing exponentially with the number of particles. However, it is of big interest to manage to describe more sufficienlty many-body interacting systems. It could lead to a better understanding of phenomena like high temperature superconductivity or QCD. Most of the problems cannot be solved exactly, hence need to be dealt with approximately. There are two common methods used in quantum mechanics (on the lattice) and QFT (in the continuum): the perturbation theory and the variational method. The first is applicable only when the interactions are weak, the second is more general, though one needs to guess a good Ansatz. In this report we will focus on the latter.

Many breakthroughs in quantum many-body physics came from proposing a suitable variational Ansatz that captures the relevant correlations for the systems under consideration. In the continuum, however, only few general Ansätze that surpass mean-field theory have been used. Finding a physically relevant parametrization for a quantum state in continuous space, especially in two or more dimensions, is a major challenge and would provide a useful tool for solving problems- analytically and computationally- in Quantum Field Theory. Mostly we are interested in investigating the ground state of a system. It turns out that ground states comprise only a small submanifold of the full Hilbert space, and exhibit highly non-generic features. A set of states, called continuous Tensor Network states, exhibits these features, thus is a variational ansatz suitable for low energy QFTs in d space dimensions. In this report we will use a subset of these states.

We start with a short summary of what has been done so far in the discrete, which worked as an inspiration for later developments in the continuum. A certain family of states, the so called *Tensor Network States* (TNS) [1, 2] has been used as a candidate for describing complex lattice quantum systems. These are an efficient parametrization of physically relevant many-body wave functions on a lattice [3, 4]. The individual tensors encode the key properties of the overall wavefunction, providing an efficient tool to understand the theoretical properties of ground states and are the basis of many powerful numerical algorithms [5]. Moreover, they are probably one of the most successful method to describe strongly correlated systems. Not only can one find the ground state and observables of a given Hamiltonian, but in many cases time evolution can be simulated [6, 7]. Overall, they are a natural language for topologically ordered systems [8, 9].

The field started with a variational approximation of the ground state of the two dimensional Ising model [10], describing a state wavefunction by a matrix product. In the 1990s, the so called *Matrix Product States*(MPS) enjoyed remarkable success, with the powerful numerical DMRG method [11, 12]. It is an iterative, variational method -uses MPS an Ansatz- that reduces effective degrees of freedom to those most important for a target state. The target state is the ground state. In the 2000s progress in generalizing the MPS construction to other scenarios was made: For higher dimensional systems with *Projected Entangled Pair States* (PEPS) as a natural generalization of MPS in 2 dimensions [13], and for critical systems with multiscale entanglement renormalization ansatz (MERA) [14, 15] and more. Meanwhile, physicists working in the field of quantum information theory brought new insights. The understanding that entanglement has an inner structure, which can be described by a Tensor Network, and that TNS obey the area law [16]- a fundamental property of ground states of local, gapped Hamiltonians [17]- where crucial points to establish the relevance of this family of states.

The first step to use the variational class based on Tensor Networks in Quantum field Theories was done in 2010 [18, 19] for one spacial dimension. The states were called *continuous Matrix Product states* (cMPS), as they are the continuous limit of the standard Matrix Product states. Those cMPS can be used as variational states to find ground states of quantum field theories, as well as to describe real-time dynamical features. They have been successfully tested on the Lieb-Liniger model, even for strong interactions.

The cMPS have been a fruitful basis for generalizations into higher dimensions. The analog of MERA states in the continuum has been found, called cMERA [20]. However, what has been done in one dimension for MPS is not easily generalizable in the case of the two dimensional PEPS, as problems with euclidean symmetry breaking and subtleties about the bond dimension emerge [21]. A good candidate state to describe low energy QFTs of local, gapped Hamiltonians in arbitrary dimensions, is the recently proposed *continuous Tensor Network state* (cTNS) [22]. It is based on a path integral over auxiliary fields [23]. However, no numerical applications on a physical system had been attempted so far. In this report we investigate a subclass of this cTNS, the gaussian cTNS, and apply a variational method to find the ground energy for certain simple models in one and two spacial dimensions.

The outline of this thesis is the following: In Chapter 1 we give an overview on the background knowledge on Tensor Network States. We focus especially on MPS in the discrete case, to explain why they are considered as physically relevant and give an examples of their successful use. Subsequently, we take the continuous limit and explain how the cMPS arise naturally as a variational class for one dimensional QFTs. In the case of PEPS the story is not as simple. We will have to define a new variational state, the continuous TNS, using a path integral over an auxiliary field.

In Chapter 2 we explain the main idea of a variational algorithm and perform the computations which will enable us to implement such an algorithm. We work on the special subset of gaussian cTNS and perform all the needed computations to express in a closed form the correlation functions and all their derivatives w.r.t. the parameters of the Tensor Network.

Chapter 3 is an application of the tools we developed in the previous Chapter, on a simple gaussian model, first in one and then in two dimensions. We compare the numerical results we get from our variational method with the analytic exact results.

Chapter 1

Theoretical Background

1.1 Tensor Network States

There are very few problems in physics which can be solved exactly, hence they need to be dealt with approximately, either with analytical or with numerical methods. There are two common methods used in quantum mechanics and QFT: perturbation theory and the variational method. Perturbation theory is useful for weakly interacting systems. The system is then studied through a power series expansion in a small parameter, i.e. the physical quantities are expressed in power series in λ. For strong interacting theories this approximation breaks down, thus other methods have to be used. Another important restriction is that the free theory, when sending λ to zero, needs to be integrable, so exactly solvable analytically.

To use a variational method, the coupling strength can be arbitrary large and there is no demand for integrability. The variational method can be more robust in situations where it is hard to determine a good unperturbed Hamiltonian. It is a useful method for finding the ground state of a given Hamiltonian. Many problems have been solved variationally, as the Bardeen–Cooper–Schrieffer (BCS) theory of supercoductivity.

The basic idea of the variational method [24] is to guess a trial wavefunction for the problem, which has adjustable parameters called variational parameters. These parameters are varied until the energy of the trial wavefunction is minimized. The resulting trial wavefunction and its corresponding energy are variational approximations to the exact wavefunction and energy. In particular, the variational principle asserts that for any state $|\psi\rangle$ in the Hilbert space $\mathcal{H}$ of a system with Hamiltonian $\hat{H}$ one finds an energy expectation value that exceeds the ground state energy,

$$\varepsilon_0 \leq \frac{\langle\psi|\hat{H}|\psi\rangle}{\langle\psi|\psi\rangle}, \tag{1.1}$$

with ε_0 the ground state energy of $\hat{H}$. If one has a variational ansatz states $|\psi(z)\rangle$, with z being the variational parameter, we try to find the value of the parameter z such that $|\psi(z^*)\rangle$ gives the lowest energy $E_0 \geq \varepsilon_0$.

The success of a variational method depends on the initial guess of the form of ground state wavefunction. Thus, a good physical intuition is required for a successful application of the variational method. Throughout the years many different variational wavefunctions as coherent states and Gaussian states, have been tried out. The most outstanding is the variational family of *Tensor Network States*(TNS), due to their numerical efficiency. Moreover, they fulfil the area law and they describe easily the entanglement structure of a system.

In order to understand this set of states we will start with their simplest form, defined in one dimension. In that case the TNS are called *Matrix Product States* (MPS). They are a natural choice for an efficient representation of 1d quantum low energy states of systems with gapped local Hamiltonians. After defining such a state and explaining its properties we will generalize to more spacial dimensions.

1.1.1 Matrix Product States (MPS)

In this section we will begin with the most generic one dimensional quantum many-body state and will decompose its wavefunction in a Matrix Product. This state, called Matrix Product state, will make us understand better the underlying physics and entanglement features of the system. In combination with a method called truncated Singular Value Decomposition, see Appendix.A. The MPS will provide us with a useful tool to perform numerical simulations, with a decreased number of parameters. There are many specific examples of non-trivial states that can be represented exactly by MPS, such as the GHZ state, the AKLT state and the $1d$ cluster state [1].

We begin with a one dimensional lattice of N sites and periodic boundary conditions. On every site there is a spin described by the state vector $|j_l\rangle$ which lives in the m dimensional Hilbert space $\mathcal{H}_l$. The most generic state of this lattice is written as a linear combination of all possible configurations

$$|\chi\rangle = \sum_{j_1,j_2,\dots j_N} C_{j_1,j_2\dots j_N}|j_1\rangle \otimes |j_2\rangle \otimes \dots \otimes |j_N\rangle, \tag{1.2}$$

The state is completely specified by the rank-N tensor C, see Appendix A. We will decompose the tensor in a matrix product by using iterative Schmidt decompositions [26].

The Schmidt decomposition Theorem states:
Let $\mathcal{H}_1$ and $\mathcal{H}_2$ be Hilbert spaces of dimensions n and m respectively. Assume $n \geq m$. For any vector w in the tensor product $\mathcal{H}_1 \otimes \mathcal{H}_2$, there exist orthonormal sets $\{u_1, \dots, u_m\} \subset \mathcal{H}_1$ and $\{v_1, \dots, v_m\} \subset \mathcal{H}_2$ such that $w = \sum_{i=1}^{m} \lambda_i u_i \otimes v_i$, where the scalars λ_i are real, non-negative and uniquely determined by w. The same can be written with Tensors, $w = \Lambda|u\rangle \otimes |v\rangle$ where Λ is the diagonal matrix with elements $\{\lambda_1, \lambda_2, \dots, \lambda_m\}$ and $|u\rangle = [u_1, u_2, \dots, u_m]^T$,$|v\rangle = [v_1, v_2, \dots, v_m]^T$.

Applying the decomposition to the first site we get

$$|\chi\rangle = \Lambda^{(1)}|v\rangle_1 \otimes |u\rangle_{[2,3,\dots N]} \tag{1.3}$$

which in the $|j\rangle$ basis writes

$$|\chi\rangle = \sum_{j_1}^{m} \Lambda^{(1)} \alpha_{j_1} |j_1\rangle \otimes |u\rangle_{[2,3,...N]} \tag{1.4}$$

We set $A^{(1)}_{j_1} = \Lambda^{(1)} a_{j_1}$, where $A^{(1)}$ is a 3 tensor describing the physics at site 1. Fixing one index, here j_1, $A^{(1)}_{j_1}$ gets a simple $m \times m$ matrix. Performing the same step for every site and taking care of the periodic boundary conditions we arrive at

$$|\chi\rangle = \sum_{j_1, j_2, ... j_N}^{m} Tr[A^{(1)}_{j_1} A^{(2)}_{j_2} \dots A^{(N)}_{j_N}] |j_1\rangle \otimes |j_2\rangle \otimes ... \otimes |j_N\rangle \tag{1.5}$$

The quantity $Tr[A^{(1)}_{j_1} A^{(2)}_{j_2} ... A^{(N)}_{j_N}]$ is a simple matrix product, which defines the state uniquely. Up to now we have done no approximation. Whatever generic state (1.2) can be written as (1.5). We factorize every matrix, performing a SVD, see eq. (A.3). One can see that usually only a certain amount of parameters in the tensor have an actual physical relevance, the ones which correspond to the larger singular values. Some of the components of the tensors correspond to zero (or approximately zero) singular values, which here are just the Schmidt weights, thus one can truncate the matrix to $D \times D$ dimensions, with $D \leq m$, using eq. (A.4). In the case where the truncated Schmidt weights are actually zero the state is still exact after truncation. If we truncate components which correspond to almost zero weights we are ending up with an approximation of the exact state. The more we truncate the worse the approximation gets, but we gain in computational speed as the parameters which describe the system are less. Note that MPS states are a complete class of quantum states and by increasing D sufficiently one can capture exactly any pure state of the system.

We now assume that A is a $D \times D \times m$ tensor of rank 3. D is the so called *bond dimension* of the tensor Network, the bigger D the bigger the tensors and the more parameters we have describing our system. As we are contracting all the indices of dimension D these indices are not variables of the system. Therefore they are called virtual indices. Thus 3-rank tensors A have one physical index, of dimension m and two (for $d = 1$) virtual indices of dimension D.

One can easily impose translational invariance. In that case the state is determined by a single tensor A

$$|\chi\rangle = \sum_{i_1, i_2 ... i_N} \mathrm{Tr}[A_{i_1} A_{i_2} ... A_{i_N}] |j_1\rangle \otimes |j_2\rangle \otimes ... \otimes |j_N\rangle. \tag{1.6}$$

An important property of a matrix product state is that it is described by very few numbers. While a general state vector of a system composed of N spin-m systems is defined by $\mathcal{O}(m^N)$ real parameters, an MPS of bond dimension D can be represented by $\mathcal{O}(mND^2)$ real parameters. For constant D, this is linear in N, as opposed to exponential in N, so this ansatz gives rise to a drastic reduction of the number of variational parameters.

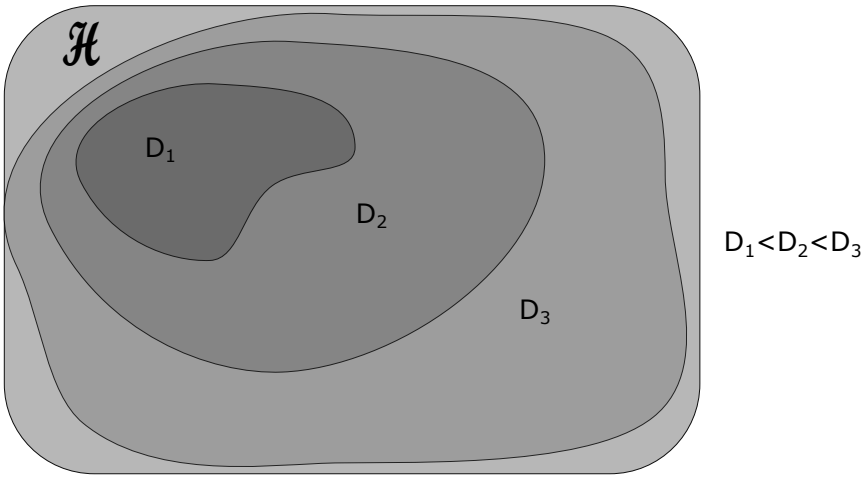

Figure 1.1: The family of MPS is complete. For finite bond dimension D cMPS are elements of a subspace $\mathcal{M}_D \in \mathcal{H}$. The larger D the larger this subspace. For $D \to \infty$ the family covers the whole space $\mathcal{H}$.

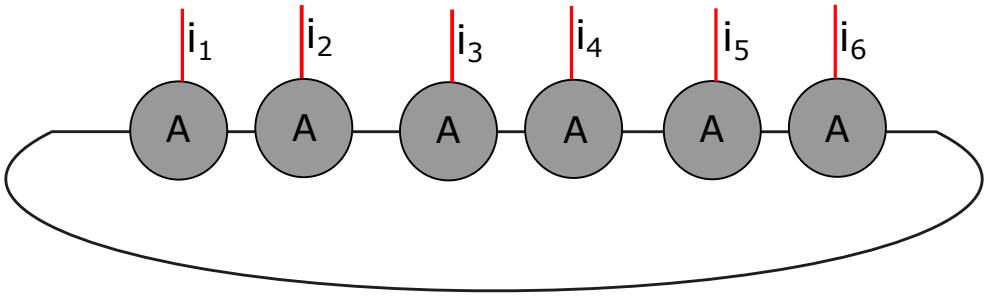

Figure 1.2: Graphical representation of an MPS, for a lattice of $N = 6$ spins. Virtual indices are in black and the physical indices in red. For better understanding of the graphical notation read Appendix A.

Correlation Functions and observables

Expectation values of local operators can be calculated exactly for an MPS. We are particularly interested in the expectation value of the two point operator $\langle\psi|\mathcal{O}_0\mathcal{O}_r|\psi\rangle$, where the subscript denotes the position the operator acts on.

One can show that the expectation value decreases exponentially in distance, $\langle\psi|\mathcal{O}_0\mathcal{O}_r|\psi\rangle \propto e^{-r/\xi}$ [5], where ξ is some finite number, such that for $r \to \infty$ we get zero correlations. ξ is called correlation length as it gives a quantitative value for how extended the correlations are in the system. For infinite ξ, i.e. in the critical regime, the correlation function does not anymore decay exponentially. Throughout the report, the decay of correlations will be often our concern, as we need our approximated two point functions to decay exponentially in distance, as long as we are far away from the critical point.

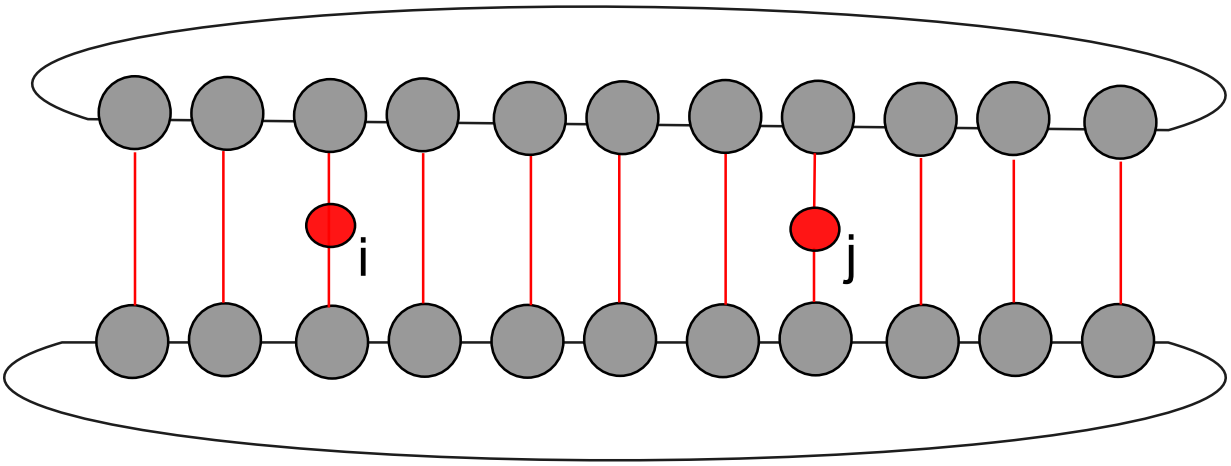

Figure 1.3: Graphical representation of the expectation value of two operators, separated by $r = j - i$ sites. Taking expectation values corresponds to contracting the physical indices.

1.1.2 Area Law

In this subsection the area law will be explained, as it is an important criterion for the physical relevance of a state. There are many reasons to believe that states of a quantum system with an energy gap ΔE and a local Hamiltonian obey an area law [17, 16]. This non-generic property makes the physical quantum states to comprise only a small submanifold $\mathcal{H}_p \subset \mathcal{H}$, as for a generic state in $\mathcal{H}$ the entanglement entropy would grow with volume.

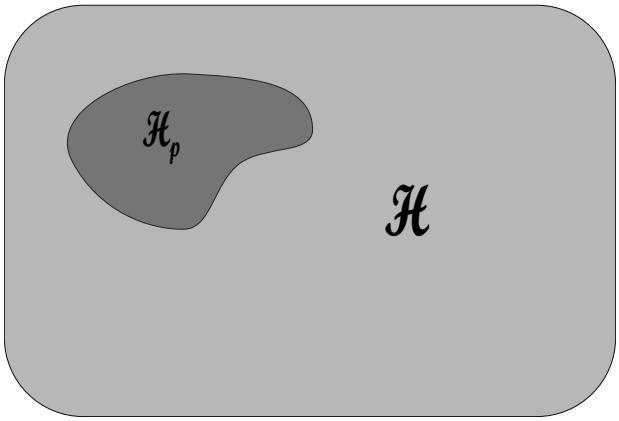

Figure 1.4: Observable states comprise only a tiny submanifold $\mathcal{H}_p \subset \mathcal{H}$, whose states exhibit nongeneric properties.

Let us suppose we split a system in two parts B and its complement B^c, see Fig. 1.5. The entanglement entropy S is defined in respect to some bipartition as

$$S = -tr[\rho_B \log_2 \rho_B] \tag{1.7}$$

where $\rho_B = tr_{\mathcal{B}^C}[|\psi\rangle\langle\psi|]$ is the reduced density matrix, $|\psi\rangle \in \mathcal{H}$. The entanglement entropy measures the amount of entanglement between the two subsystems. It is zero if the state ρ_B is pure. If the to systems are entangled the reduced density matrix ρ_B corresponds to a mixed state. Now the area law states that the entanglement entropy grows at most proportionally with the boundary ∂B between the two partitions, so $S_{max} \propto |\partial\mathcal{B}|$.

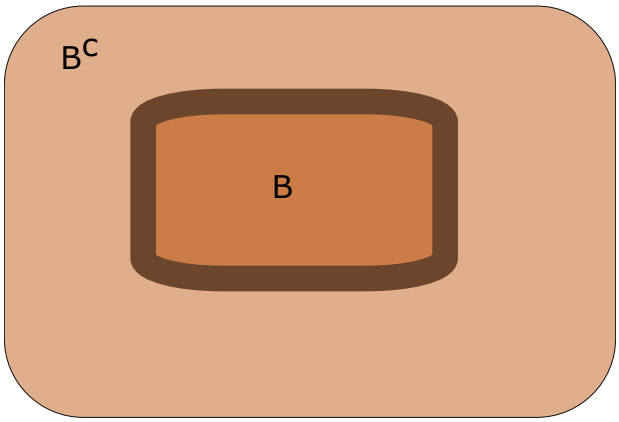

Figure 1.5: Bipartite system

Matrix Product states are a family of states which satisfy the area law. In one dimension the boundary of the subsystem consists of two sites independent of the particle number N, see Fig.1.6. One can show that the entanglement entropy of an MPS is bounded by $S_{max} = \mathcal{O}(\log_2(D))$, where D is the bond dimension of the tensors. That means that

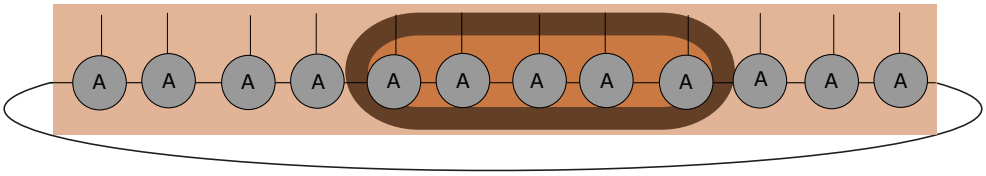

Figure 1.6: Bipartition of an MPS

the bound is independent of the system size. The behaviour of the entanglement scaling is therefore the same for MPS as for ground states of gapped models. Moreover, the bond dimension turns out to be a quantitative measure of the entanglement present in the quantum state. For example for $D = 1$ we have a separable product state, so all the particles are independent, whereas $D > 1$ provides non trivial entanglement properties.

A question which may arise is how well an MPS approximates a naturally occurring state. It was shown by Hastings [27] the error in approximating the ground state by a matrix product state of bond dimension D scales as $D^{-1/\xi}$, where ξ is the correlation length. For a finite ξ the approximation gets better when we increase D. Moreover, the approximation works well when ξ is small, so for short range correlations, which arise from finite, local Hamiltonians. As one reaches the critical point, i.e. the gap is closing and the correlation length is exploding, the MPS is not anymore describing the system as

efficiently. Thus, for $\Delta E \to 0$ we need higher bond dimensions to compensate. We will see an illustration of this later.

1.1.3 Projected Entangled Pairs State (PEPS)

The MPS class has provided a fruitful basis for generalizations. It has inspired several powerful extensions to higher dimensions and different geometries. The idea is the same as for $d = 1$, only that now we have a lattice of $N \times N$ sites. The state

$$|\chi\rangle = \sum_{i_1, i_2 \ldots i_{N^2}} c_{i_1 \ldots i^{N^2}} |i_1 i_2 \ldots i_{N^2}\rangle. \tag{1.8}$$

is fully characterized by the tensor $c_{i_1 \ldots i^{N^2}}$. This tensor can be replaced by a network of interconnected tensors with fewer coefficients, in analogy with the 1 dimensional case. Though, in 2 dimensions there are many different ways to connect the Tensors. In order to avoid lengthy formulas and confusing index-contractions, Tensor Network notation is used, see Appendix A. Some examples of different tensor networks in 2 dimensions are given in the literature [2].

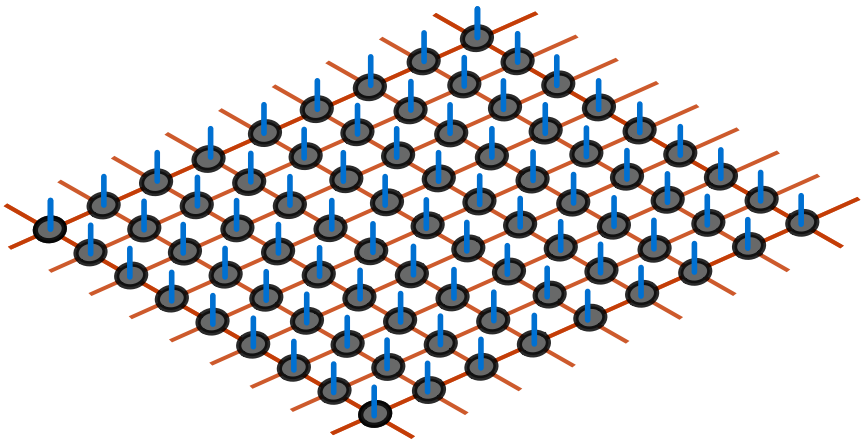

Figure 1.7: PEPS on a square lattice

The tensor decomposition we choose defines the variational class of the state. Depending on the lattice geometry we describe different physics. We want our system to be translational invariant and to fulfil the area law, as we want to parametrize a ground state. Thus, we choose the simplest structure which fulfils these requirements, the square lattice, see Fig. 1.7. Now the tensors are 5-rank, with 4 virtual D dimensional indices (blue) and one physical one (red). The states are called Projected Entangled Pair States (PEPS) [13].

The way the virtual indices are contracted provides a structure of the many body entanglement of the quantum state. For example contracting only nearest neighbor sites describes a system with only short range interactions, hence we have maximally entangled pairs. To describe physics with large correlation lengths one would need to connect sites which are far apart.

There are many specific examples of non-trivial problems that have been solved exactly by PEPS, such as the Toric Code model, the $2d$ Resonating Valence Bond State, the $2d$ AKLT state and the $2d$ cluster state [1].

Thus, Tensor Network states are mathematical representations of quantum many-body states fully characterized by a Tensor Network. The individual tensors encode the key properties of the overall wavefunction and the Tensor Network geometry is based on the entanglement structure of the system. The symmetries of the physical system impose symmetries on the tensors.

So far, everything in this report has been restricted to the lattice setting. To study continuous quantum system with these tools one would discretize the space and make use of a variational method on the lattice. The goal of the next two sections is to explain how to avoid the discretization and how to apply these variational methods directly in the continuum.

1.2 Continuous Matrix Product States (cMPS)

An important challenge is the generalization of Tensor Networks from lattice to continuous systems, which would allow the direct study of quantum field theories. The ansatz formulated in the continuum would not require an underlying lattice approximation. This is useful because the continuum provides a whole range of exact and approximate analytic techniques, as Gaussian functional integrals. In the continuum the states are called continuous Matrix Product states (cMPS), and in analogy with the standard MPS they are expected to be both an computationally efficient and complete set of states.

We consider a one dimensional system of bosons with periodic boundary conditions, associated with field operators $\psi(x) \in \mathcal{H}$ with canonical commutation relations, $[\psi(x), \psi^\dagger(y)] = \delta(x-y)$ and $0 \leq x, y \leq L$ continuous space coordinates. $|\Omega\rangle$ is the vacuum state of the physical Hilbert space $\mathcal{H}$, with $\psi(x)|\Omega\rangle = 0$ for $\forall x \in [0, L]$. The complete family of cMPS is defined as [18]:

$$|\chi\rangle = \mathrm{Tr}_{\mathrm{aux}}[\mathcal{P}e^{\int_0^L dx[Q(x)\otimes\mathbb{1}+R(x)\otimes\psi^\dagger(x)]}]|\Omega\rangle \tag{1.9}$$

with $Q(x), R(x)$ position dependent complex $D \times D$ matrices, that act on a D dimensional auxiliary space $\mathcal{H}_{\mathrm{aux}} \in \mathbb{C}^D$, $\mathrm{Tr}_{\mathrm{aux}}$ the trace over the auxiliary system. We will see that D corresponds to the bond dimension we have seen in the discrete case. In a translational invariant system Q and R do not depend on the position. $\mathcal{P}exp$ is the path ordered exponential, which will be explained in the next paragraph. The Langrangian $\mathcal{L}(x) = [Q(x) \otimes \mathbb{1} + R(x) \otimes \psi^\dagger(x)]$, has to be invariant under the symmetries of the system.

We try to gain some intuition into what these states describe, by discretizing the space and stressing the meaning of the sites at which a particle is created. First, we split the space $[0, L]$ into N equal length ϵ paths. The path-ordered exponential appearing in eq.(1.9) is then simply

$$\mathcal{P}e^{\int_0^L dx\mathcal{L}(x)} = \lim_{\epsilon\to 0}\left[e^{\epsilon\mathcal{L}(u_N)}e^{\epsilon\mathcal{L}(u_{N-1})}...e^{\epsilon\mathcal{L}(u_1)}\right],$$

where u_j is the position of site $j = 1, 2 \ldots N$. Next, we expand $e^{\epsilon S(x)}$ and get

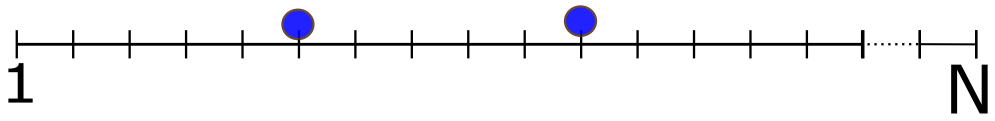

Figure 1.8: Partition in N sites. Example case for n=2, such that $|\chi\rangle = \mathrm{Tr}_{\mathrm{aux}}[\lim_{\epsilon\to 0} \mathcal{P}e^{\int_{x_{11}}^{x_N} Q(x)dx} e^{\epsilon R(x_{11})\otimes\psi(x_{11})} \mathcal{P}e^{\int_{x_6}^{x_{11}} Q(x)dx} e^{\epsilon R(x_6)\otimes\psi(x_6)} \mathcal{P}e^{\int_0^{x_6} Q(x)dx}|\Omega\rangle$

$$|\chi\rangle = \sum_{n=0}^{\infty} \int_{0<x_1<x_2<\ldots<x_n<L} dx_1 dx_2 \ldots dx_n \phi_n \psi^\dagger(x_1)\psi^\dagger(x_2)\ldots\psi^\dagger(x_n)|\Omega\rangle \tag{1.10}$$

where n is the particle number and x_i the positions of the particles with $i = 1, 2 \ldots n$, which of course coincide with some of the u_j. The wavefunction is given by

$$\phi_n = \mathrm{Tr}_{\mathrm{aux}}[u_Q(0, x_1)R(x_1)u_Q(x_1, x_2)R(x_2)\ldots R(x_n)u(x_n, L)] \tag{1.11}$$

where $u_Q(x, y) = \mathcal{P}\exp[\int_x^y Q(x)dx]$. Equation (1.10) shows that an MPS can be interpreted as a superposition over the different particle number sectors in the Fock space. u_Q can be interpreted as a propagator, while R can be understood as a scattering matrix that creates a physical particle.

To make that more explicit for the reader we compute the wave function representation in an example case, for two particles $n = 2$ distributed on a lattice of N sites, see Fig.1.8. In this specific case where the positions of the particles is fixed the state gets

$$\begin{aligned}|\chi(x_1 = u_6, x_2 = u_{11})\rangle_{n=2} = \mathrm{Tr}_{\mathrm{aux}}[\lim_{\epsilon\to 0} &\mathcal{P}e^{\int_{x_{11}}^{x_N} Q(x)dx} e^{\epsilon R(x_{11})\otimes\psi(x_{11})} \\ &\mathcal{P}e^{\int_{x_6}^{x_{11}} Q(x)dx} e^{\epsilon R(x_6)\otimes\psi(x_6)} \mathcal{P}e^{\int_0^{x_6} Q(x)dx}|\Omega\rangle,\end{aligned}$$

but of course in order to get the most generic state with two particles one has to integrate over the positions $|\chi\rangle_{n=2} = \int dx_1 dx_2 |\chi(x_1, x_2)\rangle_{n=2}$.

1.2.1 Correlation functions and expectation values

We are interested in computing some expectation values of normal ordered observables $\langle\chi(\overline{Q}, \overline{R})| : \mathcal{O}[\{\psi^\dagger\}, \{\psi\}] : |\chi(Q, R)\rangle$, particularly the correlation function and the energy. As the states themselves depend on the matrices Q and R, so will the observables. As we are in a Field Theory the easiest way usually is proceeding by using a generating functional

$$Z[\{\overline{J}\}, \{J\}] = \mathrm{Tr}\left[e^{L\mathbb{T}}\mathcal{P}\exp\{\int_{-L/2}^{L/2} dx J(x)[R\otimes\mathbb{1}_D] + \overline{J(x)}[\mathbb{1}_D\otimes\overline{R}]\}\right] \tag{1.12}$$

where $\mathbb{T} = Q\otimes\mathbb{1}_D + \mathbb{1}_D\otimes\overline{Q} + R\otimes\overline{R}$ is coming from the fact that the state is not normalized. Now we compute the two point function,

$$\langle\chi(\overline{Q}, \overline{R})|\psi^\dagger(x)\psi(y)|\chi(Q, R)\rangle = \frac{\delta}{\delta\overline{J(y)}}\frac{\delta}{\delta J(x)} Z[\{\overline{J}\}, \{J\}]|_{j,\overline{J}=0} \tag{1.13}$$

which simply, for $x < y$, takes the form

$$\langle\chi(\overline{Q},\overline{R})|\psi^\dagger(x)\psi(y)|\chi(Q,R)\rangle = \mathrm{Tr}\left[e^{(x+L/2)\mathbb{T}}(R\otimes\mathbb{1}_D)\mathcal{P}e^{(y-x)\mathbb{T}}(\mathbb{1}_D\otimes\overline{R})\mathcal{P}e^{(L/2-y)\mathbb{T}}\right]$$

One can check that the real part of the eigenvalues of $\mathbb{T}$, is finite and non positive. Thus, for growing distance $|x-y|$ the exponential $e^{(y-x)\mathbb{T}}$ is decreasing exponentially. The realization that the correlation function is decreasing exponentially with distance is essential, for the MPS to describe efficiently a system of a gapped Hamiltonian. On the other hand, it is impossible to describe a system at the critical point.

The density operator at point x is given by

$$\langle\chi(\overline{Q},\overline{R})|\psi^\dagger(x)\psi(x)|\chi(Q,R)\rangle = \mathrm{Tr}[e^{L\mathbb{T}}(R\otimes\overline{R})] \tag{1.14}$$

To compute the energy one needs to take the expectation value of the Hamiltonian

$$E = \langle\hat{H}\rangle = \langle\hat{T}\rangle + \langle\hat{V}\rangle \tag{1.15}$$

where $\langle\hat{T}\rangle = \langle\chi(\overline{Q},\overline{R})|\left(\frac{d}{dx}\psi^\dagger(x)\right)\left(\frac{d}{dx}\psi(x)\right)|\chi(Q,R)\rangle$ is the kinetic energy and $\langle\hat{V}\rangle$ the interaction energy. The last term can contain the density operator of eq.(1.14), or higher order interactions, expressed in terms of higher order moments. For example, a four point interaction term could be $\hat{V} = \int_{-L/2}^{L/2} v(x-y)\psi^\dagger(x)\psi^\dagger(y)\psi(y)\psi(x)$ and one needs to compute begineqnarray

$$\langle\chi(\overline{Q},\overline{R})|\hat{V}|\chi(Q,R)\rangle = \langle\chi(\overline{Q},\overline{R})|\psi^\dagger(x)\psi^\dagger(y)\psi(y)\psi(x)|\chi(Q,R)\rangle. \tag{1.16}$$

That way, one finds the variational value of the energy $E = E(Q,R)$. Note that no further approximation has been done.

1.2.2 Link with discrete MPS

Now we will show how these continuous MPS can be understood as a limit of a family of discrete MPS. Again we consider a tranlational invariant system of bosons of length L with periodic boundary conditions. We approximate the continuum $[-L/2, L/2]$ by a lattice with spacing ϵ and $N = L/\epsilon$ sites. We reconstruct the continuum by taking $\epsilon \to 0$. On every site we can create and annihilate particles with the creation and annihilation operators $a_i^\dagger$ and a_i, which fulfill the commutation relation $[a_i, a_j^\dagger] = \delta_{ij}$. We can relate them to the field operators $\psi(x)$ by

$$a_n = \int_{n\epsilon}^{(n+1)\epsilon} \psi(x)dx \tag{1.17}$$

and its hermitian conjugate. The field operators need to satisfy the commutation relation $[\psi(x), \psi^\dagger(y)] = \delta(x-y)$. If we define a rescaled annihilation operator $\hat{\psi}_i$ as

$$\hat{\psi}_i = \sqrt{\epsilon}a_i \tag{1.18}$$

which fulfils

$$[\hat{\psi}_i, \hat{\psi}_j^\dagger] = \frac{\delta_{ij}}{\epsilon} \tag{1.19}$$

in the limit $\epsilon \to 0$ we regain $\psi_i \to \psi(x)$. Now we can define a family of translational invariant MPS on a discretized lattice as

$$|\chi_\epsilon\rangle = \sum_{i_1 \ldots i_N} Tr[A_{i_1} \ldots A_{i_N}](\hat{\psi}_1^\dagger)^{i_1} \ldots (\hat{\psi}_N^\dagger)^{i_N}|\Omega\rangle. \tag{1.20}$$

This is the same state as defined in eq.(1.6), for $|j_l\rangle = (\psi_l^\dagger)^{j_l}||\Omega\rangle$. We will take $\epsilon \to 0$ and $n \to \infty$ such that the particle density ρ stays constant. Under this condition it is highly unlikely for two particles to be at the same point. Thus we will make the assumption that $i = 0$ or 1. We choose the matrices $A = A(Q, R)$ to depend on the matrices R and Q, in such a way that as $\epsilon \to 0$ the limit of the state is well defined and we get the cMPS of eq. (1.10):

$$A_0 = \mathbb{1} + \epsilon Q \tag{1.21}$$

$$A_1 = \epsilon R \tag{1.22}$$

$$A_n = \epsilon^n \frac{R^n}{n!}, \tag{1.23}$$

We are in the special case where we restrict to a finite particle density, most of the sites are empty in the limit and A^0 is the dominant matrix.

The correspondence of cMPS with MPS is important, because they most likely inherit all the properties of an MPS, like the fact that the entanglement entropy is bounded from above by $2log_2(D)$, see sec.1.1.2.

1.2.3 Application on the Lieb-Liniger Model

The cMPS have been successfully used as a variational ansatz for strongly correlated continuous theories, for example to find the ground state energy of the Lieb-Liniger model [28], which describes non relativistic bosons in an one dimensional space interacting via a contact potential

$$H = \int_{-\infty}^{\infty} \left[\frac{d\psi^\dagger}{dx} \frac{d\psi}{dx} + c\psi^\dagger(x)\psi^\dagger(x)\psi(x)\psi(x) \right]. \tag{1.24}$$

The goal was to approximate the ground state energy density by variational methods using MPS and compare it with the exact analytical solution and Monte Carlo algorithms [18]. For the first we need to use the expressions $\langle\psi\psi\rangle$ computed in section 1.2.1. As the system is solvable analytically, using the Bethe Ansatz, a comparison is possible. The energy density is finite and can be expressed as $\rho^3 e(c/\rho)$, where ρ is the density and $e(c/\rho)$ the energy density at $\rho = 1$. For $c = 2$ the Bethe ansatz gives $e = 1.0504$ and the Monte Carlo Method $e = 1.0518$. With the cMPS variational method one obtains a different energy density for different bond dimensions. One expects the method to approximate the actual lowest energy state better for bigger bond dimensions, thus the actual lowest energy

density to be approximated better. In fact, $e_{MPS} = 1.1241, 1.0618, 1.0531, 1.0515, 1.0512$ and 1.0508 for $D = 2, 4, ..12$ bond dimensions, see Fig.1.9. So with little numerical effort one can obtain results comparable to those of Monte Carlo methods.

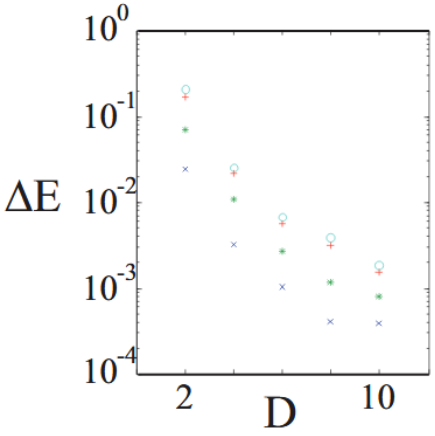

Figure 1.9: The relative error $\Delta E = (e - e_{Bethe})/e_{Bethe})$ (where e_{Bethe} is the energy given by the Bethe Ansatz solution) as a function of D for $c = 0.2, 2, 20$ and 200 (x,*,+, and o, respectively) [18].

An important fact is that the cMPS methods do not rely on the fact that the model is integrable. So one could apply the same method to models which are not solvable analytically. Another important result was that even for big c, for example $c = 200$, so for strongly interacting bosons, the results were still good. In this region perturbative methods are not applicable, so the importance of this variational method becomes clear The relative error was bigger for bigger c, but by increasing the bond dimension sufficiently one can approximate the lowest energy state sufficiently.

Thus, in the one dimensional case the cMPS variational ansatz is efficient to find the lowest energy state of a system. In this report we will try to check if the same holds for higher dimensions, using instead of cMPS another variational class, the continuous Tensor Network States, which will be described in the next section.

1.3 Continuous Tensor Networks States (cTNS)

The generalization of continuous Matrix Product States to $d \geq 2$ spatial dimensions is called continuous Tensor Networks States (cTNS). As before the continuous TNS allow the direct study of quantum field theories, without the prior need of discretizing space. Following the same ideas as in the previous section, one would simply take the continuum limit of a TNS, by letting the lattice spacing go to zero, while appropriately rescaling the tenors. In the case of $d = 1$, we showed that this is working, see sec. 1.2.2. For $d \geq 2$ though, the situation is less trivial and a naive extension can lead to a breaking of Euclidean symmetries. A way to treat the problem is exploiting the similarity between a

tensor contraction over the indices lying on the links of a tensor network and a functional integral over a field living on the continuum limit of this construction, as explained in Appendix B.

We begin with the definition of a cTNS for bosonic quantum fields in the functional integral formulation, as it is defined in [22]:

$$|V,a\rangle = \int \mathcal{D}\phi \exp\left(-\int_\Omega d^d x \frac{1}{2}\sum_{k=1}^{D}[\nabla\phi_k(x)]^2 + V[\phi(x)] - a[\phi(x)]\psi^\dagger(x)\right)|0\rangle \tag{1.25}$$

The state describes bosons in d spacial dimensions and periodic boundary conditions. The physical Fock vacuum state is noted as $|0\rangle$. We have two sorts of field operators, the physical bosonic ones, which fulfil the commutation relation $[\psi(x),\psi^\dagger(y)] = \delta^d(x-y)$ and the auxiliary fields, which are D dimensional vectors, $\phi = \{\phi_k\}_{k=1}^D$, being integrated over in the path integral. D is the continuous equivalent of bond dimensions, and is called *bond-field dimension*. Here, we choose a and V such that they do not depend explicitly on the position, since we restrict ourselves to translational invariant systems.

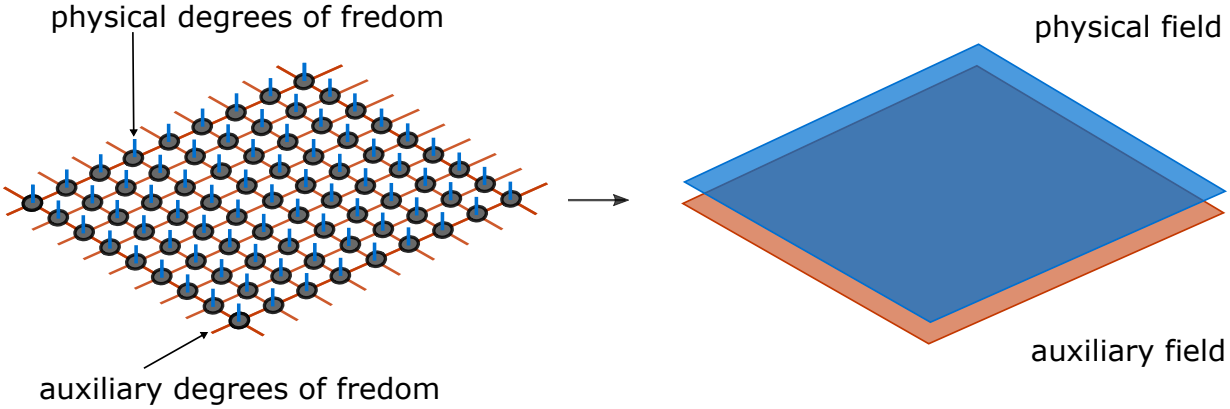

Figure 1.10: Functional integral representation – In the discrete (left) a tensor network state is obtained from a contraction of auxiliary indices connecting the elementary tensors with each other and with a boundary tensor. In the continuum (right), the contraction is replaced by a functional integral and the auxiliary indices by fields ϕ. [22]

To gain some physical understanding of these states it is convenient to express them as a generalization of bosonic field coherent states

$$|V,a\rangle = \int d\mu(\phi)\mathcal{A}_V(\phi)|a(\phi)\rangle \tag{1.26}$$

where

$$|a(\phi)\rangle = \exp\left(\int_\Omega d^d x a[\phi(x)]\psi^\dagger(x)\right)|0\rangle \tag{1.27}$$

is the unnormalized field coherent state, which specifies the occupation number of the particles in FOck space,

$$\mathcal{A}_V(\phi) = \exp\left(-\int_\Omega d^d x V[\phi(x)]\right) \tag{1.28}$$

a complex amplitude and

$$d\mu(\phi) = \mathcal{D}\phi \exp\left[-\frac{1}{2}\int_\Omega \sum_{k=1}^{D} [\nabla\phi(x)]^2\right] \tag{1.29}$$

the massless free probability measure of the auxiliary field. For a constant auxiliary field $\phi(x) = \phi$ the cTNS simplifies to a simple bosonic coherent state. That is the case when $\mathcal{A}$ is nonzero only for one mode. The measure $d\mu(\phi)$ suppresses the large momentum modes and the amplitude term is bigger in the regions the potential is smaller. In case the field is massless, we get $\mathcal{A} = 1$.

1.3.1 Correlation functions and expectation values

Just as in Section 1.2.1 we are interested in computing observables, as the correlation functions and the energy of a given Hamiltonian. In order to compute them, we first introduce the generating functionals

$$Z_{j',j} = \frac{\langle V, a| \exp(\int d^d x j'(x)\cdot\psi^\dagger(x) \exp(\int d^d y j(y)\cdot\psi(y))|V,a\rangle}{\langle V,a|V,a\rangle} \tag{1.30}$$

which we use to compute the two point functions

$$\langle\psi^\dagger(x)\psi(y)\rangle = \frac{\delta}{\delta j'(x)}\frac{\delta}{\delta j(y)} Z_{j',j}|_{j',j=0}, \tag{1.31}$$

$$\langle\psi(x)\psi(y)\rangle = \frac{\delta}{\delta j(x)}\frac{\delta}{\delta j(y)} Z_{j',j}|_{j',j=0} \tag{1.32}$$

and

$$\langle\psi^\dagger(x)\psi^\dagger(y)\rangle = \frac{\delta}{\delta j'(x)}\frac{\delta}{\delta j'(y)} Z_{j',j}|_{j',j=0}. \tag{1.33}$$

but one can take higher order functional derivatives to obtain higher order momenta, like four point functions.

We expect the two point function $\langle\psi^\dagger(x)\psi(y)\rangle$ to decay exponentially in distance and $\langle\psi^\dagger(x)\psi(x)\rangle$ to be positive and finite as it expresses the density of the particles at position x, but we will come back to that when we actually perform the computations in the two next Chapters of this report.

For a given Hamiltonian $\hat{H}$ we can compute the energy as a function of V and a. To do so we express it as $E = \langle\hat{H}\rangle = \langle\hat{T}\rangle + \langle\hat{V}\rangle$, where the interaction operator can

include terms of the form $\langle\psi^\dagger(x)\psi(x)\rangle$, $\langle\psi^\dagger(x)\psi^\dagger(x)\rangle$, $\langle\psi(x)\psi(x)\rangle$ (two point functions) and $\langle\psi^\dagger(x)\psi^\dagger(y)\psi(y)\psi(x)\rangle$ (four point function) or higher. Of course $\langle\hat{V}\rangle \in \mathbb{R}$, as it is a physical observable. The kinetic term is $\langle\hat{T}\rangle = \langle\left(\frac{d}{dx}\psi^\dagger(x)\right)\left(\frac{d}{dx}\psi(x)\right)\rangle \in \mathbb{R}$. For models which are known to have finite energy densities it is important that the expression we get for $E(V,a)$ is finite too. Note that all the expectation values so far have been expressed in real space.

To compute the generating functional one uses the Baker-Campell- Hausdorf formula. We obtain

$$Z_{j',j} = \frac{1}{\mathcal{N}}\int d\mu(\phi')d\mu(\phi) \times e^{\int_\Omega V^*[\phi'(x)]+V[\phi(x)]-a^*[\phi(x)]\cdot a[\phi(x)]-j\cdot a[\phi(x)]-j'\cdot a[\phi'(x)]} \tag{1.34}$$

where $\mathcal{N} = \langle V,a|V,a\rangle$ and $d\mu(\phi)$ is given in (1.29). This integral is solvable analytically only if it is gaussian. That restricts the form of the functions V and a for our applications. We will have to choose them such that the last integral is at most quadratic in ϕ. Already in this case we will see that the computations are quite tideous.

1.3.2 Restriction to Gaussian cTNS (GCTNS)

In our applications we will consider only a subclass of the cTNS, with which we can compute the closed formulas of expectation values: the Gaussian continuous Tensor Network States (GCTNS), see Fig.1.11. A TNS is Gaussian if it is at most second order in ϕ. In this case the most general form the functions $V[\phi(x)]$ and $a[\phi(x)]$ can have are respectively

$$V[\phi(x)] = V^{(0)} + V^{(1)}_k\phi_k + V^{(2)}_{kl}\phi_k\phi_l, \tag{1.35}$$

$$a[\phi(x)] = a^{(0)} + a^{(1)}_k\phi_k, \tag{1.36}$$

where Einstein summation is implied. We will simplify even more taking

$$a^{(0)} = V^{(1)} = 0 \tag{1.37}$$

and for simplicity we will write $a^{(1)} = a$, and $V^{(2)} = V$ so the generic form of the GCTNS in the functional integral representation is

$$|V,a\rangle = \int D\phi exp\left\{\int d^dx(-\frac{1}{2})\phi(x)(-\nabla^2+V)\phi(x) + a(x)\phi(x)\psi^\dagger(x)\right\}|0\rangle. \tag{1.38}$$

where V is a $D\times D$ dimensional matrix and a is a D dimensional vector. When integrating out the ϕ field it becomes obvious why this state is Gaussian

$$|V,a\rangle \propto exp\left\{\int d^dxd^dy\frac{1}{2}\psi^\dagger(x)a^T(-\nabla^2+V)^{-1}(x-y)a\psi^\dagger(y)\right\}|0\rangle. \tag{1.39}$$

One can check that if one takes higher order terms in a or V the generating functional (1.34) will include ϕ^3 or even higher order terms in the exponential. But it is impossible

to solve a non gaussian integral. Thus, if we take non gaussian cTNS we cannot compute the closed form of the expectation values, which are essential for our method.

We will use this parametrization to approximate the ground state of a given Hamiltonian. But let us first discuss wheather a Gaussian state is a good approximation. We know that for Hamiltonians which are at most quadratic in the creation and annihilation operators, the ground state is a Gaussian State. But for more generic Hamiltonians the ground state does not have to be Gaussian. However, in some cases a Gaussian state is still some good approximation of the actual ground state [33].

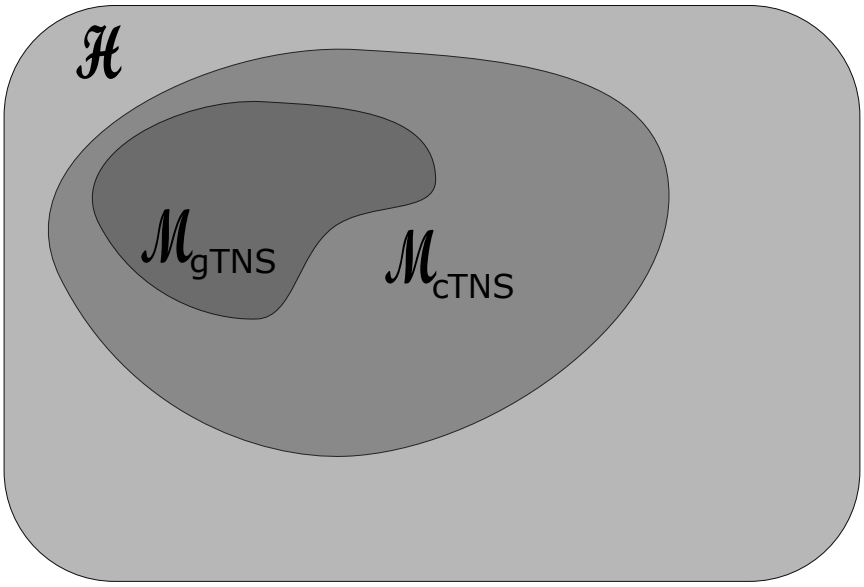

Figure 1.11: For a finite D the manifold of cTNS $\mathcal{M}_{cTNS}$ is a subspace of the full Hilbert space $\mathcal{H}$, and the space of GCTNS $\mathcal{M}_{GCTNS}$ is a subspace of $\mathcal{M}_{cTNS}$.

Chapter 2

Algorithm and Analytic Computations

In this chapter we will work exclusively with Gaussian continuous Tensor Network States. The goal is to compute the analytic closed forms of expectation values and their derivatives, which we need in order to implement the variational algorithm explained below.

2.1 Algorithm

So let us first understand what the algorithm is computing. It optimizes the variational parameters of our state such that we arrive at the lowest energy state, within our parametric class.

Essential for applying the variational method [24] is to guess a trial wavefunction for the problem, which has adjustable parameters called variational parameters. These parameters are varied until the energy of the trial wavefunction is minimized. The resulting trial wavefunction and its corresponding energy are variational approximations to the exact wavefunction and energy. In particular, the variational principle asserts that for any state $|\psi\rangle$ in the Hilbert space $\mathcal{H}$ of a system with Hamiltonian $\hat{H}$ one finds an energy expectation value that exceeds the ground state energy,

$$\varepsilon_0 \leq \frac{\langle\psi|\hat{H}|\psi\rangle}{\langle\psi|\psi\rangle}, \tag{2.1}$$

with ε_0 the ground state energy of $\hat{H}$. If one has a variational ansatz states $|\psi(z)\rangle$, with z being the variational parameter, we try to find the value of the parameter z such that $|\psi(z^*)\rangle$ gives the lowest energy $E_0 \geq \varepsilon_0$.

Now we need to choose an efficient method in order to get the correct parameter values. One could compute them analytically in a simple problem, by simply looking for the minima of the energy function w.r.t. the parameters. But in most cases it is too hard, especially for big D. Numerically the easiest way to solve the problem is with some variational algorithm. There are many efficient algorithms known to solve these sort of problems, but the main

idea can be captured with a simple gradient descent method. The gradient descent method is a first order iterative optimization algorithm to find the minimum of a function. In every iteration the algorithm optimizes the value of the parameters following the descent of the function to optimize.

In our case this function is the energy, $E = \langle V, a|H|V, a\rangle$. The variational parameters are the coefficients of the matrix V and the vector a. Let us suppose that x is a $4D$ vector with components all the parameters of out state $|V, a\rangle$. The equation which states how the parameter x^b is changing in one step is given by

$$x^b_{n+1} = x^b_n - r\frac{dE}{dx^b}$$

where r i the iteration step and we compute

$$\frac{dE}{dx^b} = \frac{d}{dx^b}\langle V, a|h|V, a\rangle - E\frac{d}{dx^b}\langle V, a|V, a\rangle$$

Note that the second term comes from the fact that our state $|V, a\rangle$ is unnormalized, $\langle V, a|V, a\rangle \neq 1$. We get

$$x^b_{n+1} = x^b_n - \left(\frac{d}{dx^b}\langle V, a|h|V, a\rangle - E\frac{d}{dx^b}\langle V, a|V, a\rangle\right). \tag{2.2}$$

In order to implement the algorithm one needs to know the closed formula for E, $\frac{dE}{dx^b}$ and $\frac{d}{dx^b}\langle V, a|V, a\rangle$, as a function of the parameters x^b.

As already seen in Section 1.3.1 we can express the energy function as a sum over different expectation values. The terms which might be included in the energy function can be very complicated, so we will restrict ourselves to compute only the ones we will need later on for our toy models, see Chapter 3, which will be $\langle\psi^\dagger(x)\psi(x)\rangle$, $\langle\psi(x)\psi(x)\rangle$ and $\langle\psi^\dagger(x)\psi^\dagger(x)\rangle$ for the interaction part and $\partial_x^2\langle\psi^\dagger(x)\psi(x)\rangle$ for the kinetic term. Subsequently, we will compute their derivatives with respect to the variational parameters. Having them we know the analytic form of $\frac{dE}{dx^b}$. In the end of this section we compute $\frac{d}{dx^b}\langle V, a|V, a\rangle$. All of these expressions are used to implement the variational code.

2.2 Correlation functions for GCTNS

In this section we compute the analytic closed forms of the two point functions, by using the generating functionals. Will will need to compute them as integrals over the momenta, $\langle\psi^\dagger(x)\psi(x)\rangle = \int \frac{d^dp}{(2\pi)^d}\langle\psi^\dagger_p\psi_p\rangle e^{ip(x-y)}$. At this point the dimensions d of the problem become relevant and one needs to check that the quantities are finite.

The generating functional from the GCTNS (1.30) is

$$Z_{j',j} = \frac{1}{N}\exp\{\int d^dx d^dy \frac{1}{2}\Lambda(j,j')^T(x)\cdot K(x,y)\cdot\Lambda(j,j')(y)\}, \tag{2.3}$$

where

$$\Lambda(j,j') = \begin{pmatrix} V - aj \\ V - a^* j' \end{pmatrix} \tag{2.4}$$

and

$$K(x-y)\begin{bmatrix} -\nabla^2 + V & -a \otimes a^* \\ -a^* \otimes a & -\nabla^2 + V \end{bmatrix} = \mathbb{1}_{2D\times 2D}\delta(x-y) \tag{2.5}$$

Using the fact that the auxiliary system is translation invariant we write $K(x,y) = K(x-y)$, which can be written in Fourrier space

$$K(x-y) = \frac{1}{(2\pi)^d}\int d^d p K(p) e^{ip(x-y)}$$

with

$$K(p) = \frac{1}{(2\pi)^d}\begin{bmatrix} p^2 + V & -a \otimes a^* \\ -a^* \otimes a & p^2 + V \end{bmatrix}^{-1} = \frac{1}{(2\pi)^d} M^{-1}(p) \tag{2.6}$$

Using (1.31), (1.32) and (1.33) we get the expressions for the two point functions as functions of V and a:

$$\langle \psi^\dagger(x)\psi(y)\rangle = \frac{1}{2}\int \frac{d^d p}{(2\pi)^d}\mathbf{a}^T K(p)\mathbf{a}^* e^{ip(x-y)} + \mathbf{a}^{*T} K(p)\mathbf{a} e^{ip(x-y)}, \tag{2.7}$$

$$\langle \psi(x)\psi(y)\rangle = \int \frac{d^d p}{(2\pi)^d}\mathbf{a}^T K(p)\mathbf{a} e^{ip(x-y)} \tag{2.8}$$

and

$$\langle \psi^\dagger(x)\psi^\dagger(y)\rangle = \int \frac{d^d p}{(2\pi)^d}\mathbf{a}^{*T} K(p)\mathbf{a}^* e^{ip(x-y)}. \tag{2.9}$$

with

$$\mathbf{a}^T = \begin{pmatrix} a_1 & a_2 & ... & a_D & 0 & 0 & 0 & ... & 0 \end{pmatrix}, \tag{2.10}$$

$$\mathbf{a}^{T*} = \begin{pmatrix} 0 & 0 & 0 & ... & 0 & a_1^* & a_2^* & ... & a_D^* \end{pmatrix}. \tag{2.11}$$

Note that $\mathbf{a}$ is a $2D$ dimensional vector now, it is not the same as a.

At this point it is important to check if the correlation function $C(x-y) = \langle \psi^\dagger(x)\psi(y)\rangle$ is decaying exponentially. As seen in the discrete case and for cMPS, this is an important property of states which describe non critical, local hamiltonians. The matrix $K(p)$ contains elements which are polynomials in p. The terms $\mathbf{a}^T K(p)\mathbf{a}^* e^{ip(x-y)}$ are of the form $\frac{A}{(p^2+B)^n}$, with $n = 1, 2 \ldots 2D$. Their fourier transform is proportional to $e^{-\sqrt{B}|x-y|}$. Thus, the correlation function decays exponentially with distance.

One can also derive the correlation functions directly in momentum space. Then, the general form of the generating functional is

$$Z_{j',j} = \frac{\langle V,a|\exp(\int \frac{d^d p}{(2\pi)^d} j'(p)\cdot\psi^\dagger(p)\exp(\int \frac{d^d p}{(2\pi)^d} j(-p)\cdot\psi(p))|V,a\rangle}{\langle V,a|V,a\rangle} \tag{2.12}$$

which for GCTNS in a translation invariant system gets

$$Z_{j',j} = \frac{1}{N}\exp\{\int \frac{d^dp}{(2\pi)^d}\frac{1}{2}\Lambda(j,j')^T(p)\cdot K(p)\cdot\Lambda(j,j')(-p)\}. \tag{2.13}$$

The correlation functions in momentum space are given by

$$\langle\psi_p^\dagger\psi_{p'}\rangle = \frac{\partial^2 Z}{\partial j'(p)\partial j(-p')} = \frac{1}{2}\left(\mathbf{a}^T K(p)\mathbf{a}^* + \mathbf{a}^{*T}K(p)\mathbf{a}\right)\delta(p-p') \tag{2.14}$$

$$\langle\psi_p\psi_{p'}\rangle = \frac{\partial^2 Z}{\partial j(-p)\partial j(-p')} = (\mathbf{a}^T K(p)\mathbf{a})\delta(p+p') \tag{2.15}$$

$$\langle\psi_p^\dagger\psi_{p'}^\dagger\rangle = \frac{\partial^2 Z}{\partial j'(p)\partial j'(p')} = (\mathbf{a}^{*T} K(p)\mathbf{a}^*)\delta(p+p') \tag{2.16}$$

As for the four-point function, using Wicks Theorem we can write it as combinations of the two point functions

$$\begin{aligned}
&\langle\psi_{p-q}^\dagger\psi_{k+q}^\dagger\psi_k\psi_p\rangle \\
&= \langle\psi_{p-q}^\dagger\psi_{k+q}^\dagger\rangle\langle\psi_k\psi_p\rangle + \langle\psi_{p-q}^\dagger\psi_k\rangle\langle\psi_{k+q}^\dagger\psi_p\rangle + \langle\psi_{p-q}^\dagger\psi_p\rangle\langle\psi_{k+q}^\dagger\psi_k\rangle \\
&= \langle\psi_{-k-q}^\dagger\psi_{k+q}^\dagger\rangle\langle\psi_k\psi_{-k}\rangle + \langle\psi_k^\dagger\psi_k\rangle\langle\psi_{k+q}^\dagger\psi_{k+q}\rangle + \langle\psi_p^\dagger\psi_p\rangle\langle\psi_k^\dagger\psi_k\rangle
\end{aligned} \tag{2.17}$$

2.2.1 Closed form of the correlation functions

In order to implement the algorithm we need to compute the closed form of the correlation functions in real space $\langle\psi^{(\dagger)}(x)\psi^{(\dagger)}(x)\rangle$ of eq.(2.7)-(2.9), which means we need to perform the integration. We know the analytic form of $K(p)$ from eq. (2.6) and now we need perform the integral over the momenta. First we diagonalize matrix $K(p)$ by diagonalizing $M(p) = p^2\cdot\mathbb{1} + U^{-1}\Lambda U$ so we get

$$K(p) = \frac{1}{(2\pi)^d}U^{-1}(p^2\cdot\mathbb{1}+\Lambda)^{-1}U, \tag{2.18}$$

where Λ is a $2D\times 2D$ diagonal matrix with eigenvalues $\lambda_1,\lambda_2,...,\lambda_{2D}$ and U is a unitary $2D\times 2D$ matrix. $M(p)$ needs to be positive definite matrix, for the state to be physical, thus $Re[\lambda_i] > 0$. The correlation function, at equal points, from (2.8) writes

$$\langle\psi(x)\psi(x)\rangle = \int\frac{d^dp}{(2\pi)^d}(\mathbf{a}^T\cdot U)(p^2\cdot\mathbb{1}+\Lambda)^{-1}(U^{-1}\cdot\mathbf{a}) = \frac{1}{(2\pi)^d}\sum_i^{2D}(\mathbf{a}^T\cdot U)_i(U^{-1}\cdot\mathbf{a})_i I_1(\lambda_i) \tag{2.19}$$

where

$$I_1(\lambda_i) = \int\frac{d^dp}{(2\pi)^d}\frac{1}{p^2+\lambda_i}$$

is an integral computed in the Appendix C. Similarly, the other correlation functions write

$$\langle\psi^\dagger(x)\psi(x)\rangle = \left[\sum_i^{2D}(\mathbf{a}^{*T}\cdot U)_i(U^{-1}\cdot\mathbf{a})_i + (\mathbf{a}^T\cdot U)_i(U^{-1}\cdot\mathbf{a}^*)_i\right] I_1(\lambda_i) \tag{2.20}$$

and

$$\langle\psi^\dagger(x)\psi^\dagger(x)\rangle = \sum_i^{2D}(\mathbf{a}^{*T}\cdot U)_i(U^{-1}\cdot\mathbf{a}^*)_i I_1(\lambda_i). \tag{2.21}$$

For the kinetic term in the Hamiltonian we need the derivative of the correlation function

$$\lim_{x\to y}\partial_x\partial_y\langle\psi^\dagger(x)\psi(y)\rangle = \left[\sum_i^{2D}(\mathbf{a}^{*T}\cdot U)_i(U^{-1}\cdot\mathbf{a})_i + (\mathbf{a}^T\cdot U)_i(U^{-1}\cdot\mathbf{a}^*)_i\right] I_{1kin}(\lambda_i) \tag{2.22}$$

where

$$I_{1kin}(\lambda_i) = \int \frac{d^2p}{(2\pi)^2}\frac{p^2}{p^2+\lambda_i}$$

is computed in Appendix C.

2.3 Computation of derivatives

2.3.1 Derivatives of correlation functions

To implement the algorithm (2.2) we need the derivative of the energy $\frac{d}{dx^b}\langle V,a|H|V,a\rangle$, where x is a vector of all the real parameters which describe our state, and $b = 1,\dots 4D$. That means we need to compute the derivatives of the correlation functions and of the kinetic term.

We start with the derivatives $\frac{\partial}{\partial x_b}\langle\psi^{(\dagger)}(x)\psi^{(\dagger)}(y)\rangle$. The derivation is similar for all of them, so we just will show the derivation steps for one. We take the derivative of eq. (2.8)

$$\frac{\partial}{\partial x_b}\langle\psi(x)\psi(y)\rangle = \int\frac{d^dp}{(2\pi)^d}\mathbf{a}^T\cdot\frac{\partial K(p)}{\partial x_b}\cdot\mathbf{a}e^{ip(x-y)} \tag{2.23}$$

where $K(p) = \frac{1}{(2\pi)^d}M^{-1}(p)$, from eq. (2.6). Using $M^{-1}M - MM^{-1} = 0$, we get that

$$\frac{\partial M^{-1}}{\partial x_b} = -M^{-1}\frac{\partial M}{\partial x_b}M^{-1} \tag{2.24}$$

For different variational parameters we get different analytical formulas. The different forms of the derivative $\frac{dM^{-1}}{dx^b}$ are computed below:

$$\frac{\partial M}{\partial Re(V_{ii})} = e_i\cdot e_i^T + e_{i+d}\cdot e_{i+d}^T$$

and

$$\frac{\partial M}{\partial Im(V_{ii})} = e_i \cdot e_i^T - e_{i+d} \cdot e_{i+d}^T$$

where e_i the $2D$ unit vector with only nonzero element the ith component. Also,

$$\frac{\partial M}{\partial Re(\mathbf{a}_j)} = -[e_j \cdot \mathbf{a}^{*T} + \mathbf{a}^* \cdot e_j^T + e_{j+d} \cdot \mathbf{a}^T + \mathbf{a} \cdot e_{j+d}^T]$$
$$\frac{\partial M}{\partial Im(a_j)} = -i[e_j \cdot \mathbf{a}^{*T} + \mathbf{a}^* \cdot e_j^T - e_{j+d} \cdot \mathbf{a}^T - \mathbf{a} \cdot e_{j+d}^T]$$

We want to perform the integral over the momenta, so again, we diagonalize $M(p) = p^2 \cdot \mathbb{1} + U^{-1}\Lambda U$ by using the unitary matrix U such that

$$-\mathbf{a}^T M^{-1} \frac{\partial M}{\partial x_b} M^{-1}\mathbf{a} = -(\mathbf{a}^T U)U^{-1}M^{-1}UU^{-1}\frac{\partial M}{\partial x_b}UU^{-1}M^{-1}U(U^{-1}\mathbf{a}) \tag{2.25}$$

Combining everything we arrive at the closed formulas. In particular, for the parameters $Re[V_{ii}], Im[V_{ii}]$ we get

$$\frac{\partial}{\partial Re[V_{ij}]}\langle\psi(x)\psi(y)\rangle = \sum_{lk}^{2d}(\mathbf{a}^T U)_l C_{lk}^+ (U^{-1}\mathbf{a})_k I_2(\lambda_l, \lambda_k),$$
$$\frac{\partial}{\partial Im[V_{ij}]}\langle\psi(x)\psi(y)\rangle = i\sum_{lk}^{2d}(\mathbf{a}^T U)_l C_{lk}^- (U^{-1}\mathbf{a})_k I_2(\lambda_l, \lambda_k).$$

and for the slightly more complicated two point function $\langle\psi^\dagger(x)\psi(x)\rangle$, we proceed similarly and get

$$\frac{\partial}{\partial Re[V_{ij}]}\langle\psi^\dagger(x)\psi(y)\rangle = -\sum_{lk}^{2d}\frac{1}{2}[(\mathbf{a}^T U)_l C_{lk}^+ (U^{-1}\mathbf{a}^*)_k + (\mathbf{a}^{*T} U)_l C_{lk}^+ (U^{-1}\mathbf{a})_k] I_2(\lambda_l, \lambda_k)$$
$$\frac{\partial}{\partial Im[V_{ij}]}\langle\psi^\dagger(x)\psi(y)\rangle = -i\sum_{lk}^{2d}\frac{1}{2}[(\mathbf{a}^T U)_l C_{lk}^- (U^{-1}\mathbf{a}^*) + (\mathbf{a}^{*T} U)_l C_{lk}^- (U^{-1}\mathbf{a})_k] I_2(\lambda_l, \lambda_k)$$

where

$$C_{lk}^\pm = -(U_{li}^{-1}U_{ik} \pm U_{l,i+d}^{-1}U_{i+d,k})$$

The integral

$$I_2(\lambda_k, \lambda_l) = \int \frac{d^d p}{(2\pi)^d}\frac{1}{p^2+\lambda_k}\frac{1}{p^2+\lambda_l}e^{ip(x-y)}$$

is computed in Appendix C.

In analogy, for the parameters $Re[a_j], Im[a_j]$ we compute

$$\frac{\partial}{\partial Re[a_j]}\langle\psi(x)\psi(y)\rangle = \sum_i^{2d} G_i j I_1(\lambda_i) + \sum_{ik}^{2d} F_{ijk}^R I_2(\lambda_i, \lambda_k)$$

and

$$\frac{\partial}{\partial Im[a_j]}\langle\psi(x)\psi(y)\rangle = i\sum_i G_i j I_1(\lambda_i) + \sum_{ik} F^I_{ijk} I_2(\lambda_i,\lambda_k)$$

with

$$G_{ij} = [U_{ji}(U^{-1}\mathbf{a})_i + (\mathbf{a}^T U)_i U_{ij}].$$

We use

$$F^R_{ijk} = -(\mathbf{a}^T U)_i (U^{-1}\frac{\partial M}{\partial Re(a_j)}U)_{ik}(U^{-1}\mathbf{a})_k,$$

$$F^I_{ijk} = -(\mathbf{a}^T U)_i (U^{-1}\frac{\partial M}{\partial Im(a_j)}U)_{ik}(U^{-1}\mathbf{a})_k$$

Also, in the case of $\langle\psi^\dagger(x)\psi(x)\rangle$ we obtain the following the derivatives in closed form

$$\frac{\partial}{\partial Re[a_j]}\langle\psi^\dagger(x)\psi(y)\rangle = \sum_i^{2d} G^+_{ij} I_1(\lambda_i) + \sum_{i,k} F^+_{ijk} I_2(\lambda_i,\lambda_k) \tag{2.26}$$

and

$$\frac{\partial}{\partial Im[a_j]}\langle\psi^\dagger(x)\psi(y)\rangle = i\sum_i G_-(\psi^\dagger\psi,i,j) I_1(\lambda_i) + i\sum_{i,k} F_-(\psi^\dagger\psi,i,j,k) I_2(\lambda_i,\lambda_k),$$

where

$$G^+_{ij} = U_{ji}(U^{-1}\mathbf{a}^*)_i + (\mathbf{a}^T U)_i U^{-1}_{i,j+d} + (\mathbf{a}^{*T} U)_i U^{-1}_{ij} + U_{j+d,i}(U^{-1}\mathbf{a})_i,$$

$$G^-_{ij} = U_{ji}(U^{-1}\mathbf{a}^*)_i - (\mathbf{a}^T U)_i U_{ij+d} - U_{j+di}(U^{-1}\mathbf{a})_i + (\mathbf{a}^{*T} U)_i U_{ij}$$

and

$$F^+_{ijk} = -[(\mathbf{a}^T U)_i (U^{-1}\mathbf{a}^*)_k + (\mathbf{a}^{*T} U)_i (U^{-1}\mathbf{a})_k](U^{-1}\frac{\partial M}{\partial Re(a_j)}U)_{ik},$$

$$F^-_{ijk} = -[(\mathbf{a}^T U)_i (U^{-1}\mathbf{a}^*)_k + (\mathbf{a}^{*T} U)_i (U^{-1}\mathbf{a})_k](U^{-1}\frac{\partial M}{\partial Im(a_j)}U)_{ik}$$

For the kinetic terms, for example $\lim_{x\to y}\frac{d}{dRe[V_{ij}]}\partial_x\partial_y\langle\psi^\dagger(x)\psi(y)\rangle$ we just need to replace the integrals of each form by their kinetic integrals, i.e. replace I_2 by I_{2kin}, see Appendix C.

Now we have all the ingredients to compute the derivative of the energy.

2.3.2 Derivatives of the norm

In this subsection the derivative of the norm we use in eq.(2.2) is computed

$$\frac{\partial}{\partial x^b}\langle V,a|V,a\rangle = \frac{\partial\langle V,a|}{\partial x^b}|V,a\rangle + \langle V,a|\frac{\partial|V,a\rangle}{\partial x^b} \tag{2.27}$$

so we need the vectors $\frac{\partial|V,a\rangle}{dx^b}$, which span the $4D$ dimensional tangent space $\mathcal{T}$ of the manifold $\mathcal{M}_{GCTNS}$.

Starting from eq. (1.38) we integrate out the auxiliary field $\phi(x)$ and obtain

$$|V,a\rangle \propto exp\left\{\int d^dx d^dy \frac{1}{2}\psi^\dagger(x)a^T(-\nabla^2+V)^{-1}(x-y)a\psi^\dagger(y)\right\}|0\rangle. \tag{2.28}$$

and in momentum space

$$|V,a\rangle \propto exp\left\{\int \frac{d^dp}{(2\pi)^d}\frac{1}{2}\psi^\dagger_p a^T\left(p^2+V\right)^{-1}a\psi^\dagger_{-p}\right\}|0\rangle. \tag{2.29}$$

The state is not normalized. We set $A(p)=p^2+V$. Now the derivatives are of the form

$$\frac{\partial|V,a\rangle}{\partial x^b} = \int \frac{d^dp}{(2\pi)^d}\frac{\partial}{\partial x^b}(\mathbf{a}^T A(p)^{-1}\mathbf{a})\psi^\dagger_p\psi^\dagger_{-p}|V,a\rangle \tag{2.30}$$

We will use the equality

$$\mathbf{a}^T\frac{\partial A^{-1}}{\partial x^b}\mathbf{a} = -\mathbf{a}^T A^{-1}\frac{\partial A}{\partial x^b}A^{-1}\mathbf{a}. \tag{2.31}$$

In particular, we have

$$\mathbf{a}^T\frac{\partial A^{-1}}{\partial Re[V_{ii}]}\mathbf{a} = -(\mathbf{a}^T A^{-1}e_i\cdot e_i^T A^{-1}\mathbf{a}), \tag{2.32}$$

$$\mathbf{a}^T\frac{\partial A^{-1}}{\partial Im[V_{ii}]}\mathbf{a} = -i(\mathbf{a}^T A^{-1}e_i\cdot e_i^T A^{-1}\mathbf{a}), \tag{2.33}$$

$$\frac{\partial \mathbf{a}^T A^{-1}\mathbf{a}}{\partial Re[a_j]} = e_j^T A^{-1}\mathbf{a} + \mathbf{a}^T A^{-1}e_j \tag{2.34}$$

and

$$\frac{\partial \mathbf{a}^T A^{-1}\mathbf{a}}{\partial Im[a_j]} = i(e_j^T A^{-1}\mathbf{a} + \mathbf{a}^T A^{-1}e_j), \tag{2.35}$$

where e_j is a unit vector with zeros at every component except for the j-th.

Again we need to compute the closed forms. Now we need to diagonalize the matrix A with the transformation W, such that for example

$$\begin{aligned}\frac{\partial}{\partial Re[V_{ii}]}(\mathbf{a}^T A^{-1}a) &= -(a^T W)(W'^{-1}A^{-1}W)(W^{-1}\frac{\partial A}{\partial Re[V_{ii}]}W)(W^{-1}A^{-1}W)(W^{-1}\mathbf{a})\\ &= -\int \frac{d^dp}{(2\pi)^d}(\mathbf{a}^T W)_k\frac{1}{p^2+\kappa_k}(W^{-1}\frac{\partial A}{\partial Re[V_{ii}]}W)_k l\frac{1}{p^2+\kappa_l}(W^{-1}\mathbf{a})_l.\end{aligned}$$

Thus, using (2.19), we get

$$\begin{aligned}\frac{\partial}{\partial Re[V_{ii}]}\langle V,a|V,a\rangle &= \int \frac{d^dp}{(2\pi)^d}\frac{\partial}{\partial Re[V_{ii}]}(\mathbf{a}^T A^{-1}\mathbf{a})\langle\psi^\dagger_p\psi^\dagger_{-p}\rangle + \text{conj}\,.\\ = -\sum_{kl}^{d}(\mathbf{a}^T W)_l(W^{-1}_{li}W_{ik})(W^{-1}\mathbf{a})_k\sum_n^{2d}(\mathbf{a}^{*T}U)_n(U^{-1}\mathbf{a}^*)_n I_3(\kappa_k,\kappa_l,\lambda_n) + \text{conj}\,.\end{aligned} \tag{2.36}$$

and

$$\frac{\partial}{\partial Re[V_{ii}]}\langle V,a|V,a\rangle = \int \frac{d^dp}{(2\pi)^d}\frac{\partial}{\partial Im[V_{ii}]}(\mathbf{a}^T A^{-1}\mathbf{a})\langle\psi_p^\dagger\psi_{-p}^\dagger\rangle + \text{conj}\,.$$
$$= -i\sum_{kl}^{d}(\mathbf{a}^T W)_l(W_{li}^{-1}W_{ik})(W^{-1}\mathbf{a})_k\sum_{n}^{2d}(\mathbf{a}^{*T}U)_n(U^{-1}\mathbf{a}^*)_n I_3(\kappa_k,\kappa_l,\lambda_n) + \text{conj}\,. \quad (2.37)$$

with the integral

$$I_3(\kappa_k,\kappa_l,\lambda_n) = \int \frac{d^dp}{(2\pi)^d}\frac{1}{p^2+\kappa_k}\frac{1}{p^2+\kappa_l}\frac{1}{p^2+\lambda_n}$$

being computed in Appendix C.

When derivating with respect to the parameters $Re[a_j]$ and $Im[a_j]$, we get

$$\frac{\partial}{\partial Re[a_j]}\langle V,a|V,a\rangle = \int \frac{d^dp}{(2\pi)^d}\frac{\partial}{\partial Re[a_j]}(\mathbf{a}^T A^{-1}\mathbf{a})\langle\psi_p^\dagger\psi_{-p}^\dagger\rangle + \text{conj}\,.$$
$$= -\sum_k\int\frac{d^dp}{(2\pi)^d}[W_{jk}(W^{-1}\mathbf{a})_k + (a^TW)_kW_{kj}^{-1}]\sum_{n}^{2d}(\mathbf{a}^{*T}U)_n(U^{-1}\mathbf{a}^*)_n I_2(\kappa_k,\lambda_n) + \text{conj} \quad (2.38)$$

and

$$\frac{\partial}{\partial Im[a_j]}\langle V,a|V,a\rangle\int \frac{d^dp}{(2\pi)^d}\frac{\partial}{\partial Im[a_j]}(\mathbf{a}^T A^{-1}\mathbf{a})\langle\psi_p^\dagger\psi_{-p}^\dagger\rangle + \text{conj}\,.$$
$$= -i\sum_k\int\frac{d^dp}{(2\pi)^d}[W_{jk}(W^{-1}\mathbf{a})_k + (a^TW)_kW_{kj}^{-1}]\sum_{n}^{2d}(\mathbf{a}^{*T}U)_n(U^{-1}\mathbf{a}^*)_n I_2(\kappa_k,\lambda_n) + \text{conj} \quad (2.39)$$

with

$$I_2(\kappa_i,\lambda_n) = \int \frac{d^dp}{(2\pi)^d}\frac{1}{p^2+\kappa_i}\frac{1}{p^2+\lambda_n}$$

computed in Appendix C.

At this point we have computed all the analytic expressions which allow us to implement a numerical computation with the gradient descent algorithm. The only thing we miss is the Hamiltonian of a model which will allow us to write down the energy as a function of the parameters V and a. This last step will be done in the next Chapter.

Chapter 3

Applications and results

In this chapter we use the analytical tools we developed in the previous chapter to check the efficiency of the variational method. The goal is to find the lowest energy state within the class of GCTNS, for a given Hamiltonian. As this is a first application of GCTNS, we need to use a model which is integrable, such that we have a benchmark.

3.1 A simple model: Exact solution

The hamiltonian density of our model is

$$\hat{h}(x) = \frac{d}{dx}\psi^\dagger(x)\frac{d}{dx}\psi(x) + \mu\psi^\dagger(x)\psi(x) + \lambda\left[\psi^\dagger(x)\psi^\dagger(x) + \psi(x)\psi(x)\right] \tag{3.1}$$

and in Fourier space

$$h_p = \left(p^2 + \mu\right)\psi_p^\dagger\psi_p + \lambda\left(\psi_p^\dagger\psi_{-p}^\dagger + \psi_p\psi_{-p}\right), \tag{3.2}$$

where ψ and $\psi^\dagger$ are the field annihilation and creation operators which fulfil the commutation relations, and $\psi|0\rangle = 0$. $|0\rangle$ is the Fock vacuum. $[\psi_p, \psi_{p'}^\dagger] = \delta_{pp'}$. $\mu > 0$ is the chemical potential, such that the energy increases when increasing the particle number. The last two terms create and annihilate pairs of bosons with opposite momenta, such that the whole system obeys momentum conservation. λ can be in general positive or negative. For small negative λ this hamiltonian can be an effective superconductivity hamiltonian.

We will work with this problem in one and two space dimensions d, in sections 3.4 and 3.5 respectively. The Hamiltonian of the model is connected to its density by

$$\hat{H} = \int_{-\infty}^{\infty} \frac{d^d p}{(2\pi)^d} h_p \tag{3.3}$$

3.2 Understanding the motivation for the model

One main reason for taking the Hamiltonian of (3.1) is that we can compute the analytic exact form of the ground state and the correlation functions. This will be useful to check

the efficiency of our method.

To understand the physical motivation for this Hamiltonian better, we will compare it with two different models and see under which conditions they coincide.

First we look at the Lieb-Liniger model [28]. The Hamiltonian density is

$$\hat{h'} = \frac{d}{dx}\psi^\dagger(x)\frac{d}{dx}\psi(x) - m\psi^\dagger\psi(x) + g\left[\psi^\dagger(x)\psi^\dagger(x)\psi(x)\psi(x)\right] \tag{3.4}$$

which describes a one dimensional gas of massive bosons, with a pointlike interaction. When we take the mean field approximation, the four point interaction $\psi^\dagger(x)\psi^\dagger(x)\psi(x)\psi(x)$ breaks down to all the possible combinations of two point interactions: $\langle\psi^\dagger(x)\psi^\dagger(x)\rangle\psi(x)\psi(x)$, $\psi^\dagger(x)\psi^\dagger(x)\langle\psi(x)\psi(x)\rangle$ and $\langle\psi^\dagger(x)\psi(x)\rangle\psi^\dagger(x)\psi(x)$. Thus, the mean field Hamiltonian of eq.(3.4) can be mapped exactly to the Hamiltonian of our model (3.1), for a certain $\mu = \mu(m, g, \langle\psi^\dagger(x)\psi(x)\rangle)$ and $\lambda = \lambda(m, g, \langle\psi^{(\dagger)}(x)\psi^{(\dagger)}(x)\rangle)$. In this case μ and λ are not independent. However, we start from the hamiltonian density of eq. (3.1) without assuming any dependence between the two constants.

The second model we will compare with is a relativistic model. We start with the massive relativistic boson (Klein-Gordon) Hamiltonian

$$\hat{H}_{KG} = \frac{1}{2}\int dx \left[\hat{\pi}^2 + \left(\frac{d}{dx}\hat{\phi}\right)^2 + m^2\phi^2\right] \tag{3.5}$$

The field operators $\hat{\phi}$ and π can be written in terms of the Fock space operators we were using throughout the report as

$$\hat{\phi} = \frac{1}{\sqrt{2\Lambda}}(\psi + \psi^\dagger) \tag{3.6}$$

$$\hat{\pi} = \frac{\sqrt{\Lambda}}{\sqrt{2}}(\psi - \psi^\dagger). \tag{3.7}$$

Now if we try to approximate the ground state with the GCTNS variational algorithm we will see that the expectation values of the kinetic term is diverging, so for big momenta the contribution of $\langle p^2\phi_p^2\rangle$ is infinite, even in one dimension. The reason is that the term contains $\langle p^2\psi_p\psi_{-p}\rangle$ and $\langle p^2\psi_p^\dagger\psi_{-p}^\dagger\rangle$ terms, which when integrated are giving infinities. That means that the algorithm will overcompensate for the high momenta region, without caring about what would optimize the correlation functions in the low momenta regions. The problem with that is that the region of interest is the lower momenta region, as the GCTNS describes systems with small entanglement entropy and decaying correlations. Thus, the fact that the algorithm will care only about the high momenta regions is overshadowing the actual physics. We want the contribution of the high momenta to be supressed. Therefore one can add a counterterm [29] of the form

$$\frac{1}{\Lambda^2}\left(\frac{d\hat{\pi}}{dx}\right)^2 \tag{3.8}$$

which removes the divergencies and serves as a momentum cutoff. The resulting Hamiltonian is of the form

$$\hat{H'}_{KG} = \int_{-\infty}^{\infty} dx \left[\frac{d}{dx}\psi^\dagger \frac{d}{dx}\psi + v_\Lambda \psi^\dagger \psi + u_\Lambda(\psi\psi + \psi^\dagger\psi^\dagger) \right] \tag{3.9}$$

with $v_\Lambda = \frac{m^2+\Lambda^2}{2}$ and $u_\Lambda = \frac{m^2-\Lambda^2}{4}$.

The resulting relativistic, regularized hamiltonian is of the same form as the hamiltonian of our model (3.1). So one can define a map between our parameters and the cutoff dependent parameters of the Klein Gordon theory

$$\mu = \frac{\Lambda^2 + m^2}{2} \tag{3.10}$$

$$\lambda = \frac{\Lambda^2 - m^2}{4}. \tag{3.11}$$

Now let us look into some special cases. If we take the mass very small $m \to 0$ we get $\mu = 2\lambda$, so that would correspond to closing the gap in our model. Thus, there is an exact mapping between a low energy theory close to the critical point and a massless relativistic theory. Another extreme case is taking the cutoff Λ to infinity. In that case $\frac{\mu}{\lambda} \to \frac{1}{2}$, for some finite mass. Thus, again this corresponds to the critical regime in our theory.

3.3 Exact Solution

In this section we will analyze the behaviour of our toy model (3.2) analytically. In the next sections we compare our GCTNS results with the exact ones obtained here.

To proceed, we diagonalize the Hamiltonian to find the eigenenergies of the excitation modes and the ground state energy. First we use the following Bogoliubov transformation

$$\psi_p = u_p b_p + v_p b^\dagger_{-p} \tag{3.12}$$

$$\psi^\dagger_p = u_p b_p + v_p b^\dagger_{-p} \tag{3.13}$$

The canonical commutation relations give

$$|u^2| - |v^2| = 1$$

without loss of generality we can set $u_p = \cosh\phi$ and $v_p = \sinh\phi$. We find that the Hamiltonian is diagonal under the condition

$$u_p v_p = \frac{\lambda}{(p^2+\mu)}(u_p + v_p) \tag{3.14}$$

and using

$$\sinh(2a) = 2\cosh(a)\sinh(a)$$
$$\cosh(2a) = \cosh^2(a) + \sinh^2(a)$$

we obtain the useful relations

$$\cosh^2(a)+\sinh^2(a)=\frac{(p^2+\mu)}{\sqrt{(p^2+\mu)^2-4\lambda^2}},$$
$$\sinh\phi\cdot\cosh\phi=-\frac{\lambda}{\sqrt{(p^2+\mu)^2-4\lambda^2}},$$
$$\cosh\phi=\sqrt{\frac{p^2+\mu}{2\sqrt{(p^2+\mu)^2-4\lambda^2}}+\frac{1}{2}}$$
$$\sinh\phi=-\sqrt{\frac{p^2+\mu}{2\sqrt{(p^2+\mu)^2-4\lambda^2}}-\frac{1}{2}}$$

In the new basis the Hamiltonian density writes

$$h_p=\epsilon(p)b_p^\dagger b_p+\epsilon_0(p) \tag{3.15}$$

where the ground state energy density is given by

$$\epsilon_0(p)=\left(p^2+\mu\right)v_p^2+2\lambda u_p v_p=\frac{1}{2}\left[\epsilon(p)-\left(p^2+\mu\right)\right] \tag{3.16}$$

and the dispersion relation by

$$\epsilon(p)=\sqrt{(p^2+\mu)^2-4\lambda^2}, \tag{3.17}$$

which is depicted in Fig.3.1. $\Delta E=\epsilon(0)=\sqrt{\mu^2-4\lambda^2}$ corresponds to the gap between the ground state and the first excited state. Our theory is well defined only for $4\lambda^2<\mu^2$. One can see that in the limit where $4\lambda^2\to\mu^2$ the excitation gap is closing. Then our system is close to the critical point and exhibits a critical behaviour. By design, with a GCTNS, we can approximate a ground state of a gapped Hamiltonian, so we will choose our model parameters such that we are far from that point. However, we will see that even close to the critical point we can capture some features of the states.

The correlation function, in the basis which diagonalizes the Hamiltonian, takes the form

$$\begin{aligned}\left\langle\psi_p^\dagger\psi_p\right\rangle&=(u_p+v_p)b_p^\dagger b_p+v_p+u_pv_p(b_pb_{-p}+b_p^\dagger b_{-p}^\dagger)\\&=\frac{(p^2+\mu)}{\epsilon(p)}b_p^\dagger b_p+\frac{\lambda}{\epsilon(p)}(b_pb_{-p}+b_p^\dagger b_{-p}^\dagger)+\left(\frac{p^2+\mu}{2\epsilon(p)}-\frac{1}{2}\right)\end{aligned} \tag{3.18}$$

Thus, in the ground state of the new basis, the correlation function is

$$\left\langle\psi_p^\dagger\psi_p\right\rangle=\left(\frac{p^2+\mu}{2\epsilon(p)}-\frac{1}{2}\right) \tag{3.19}$$

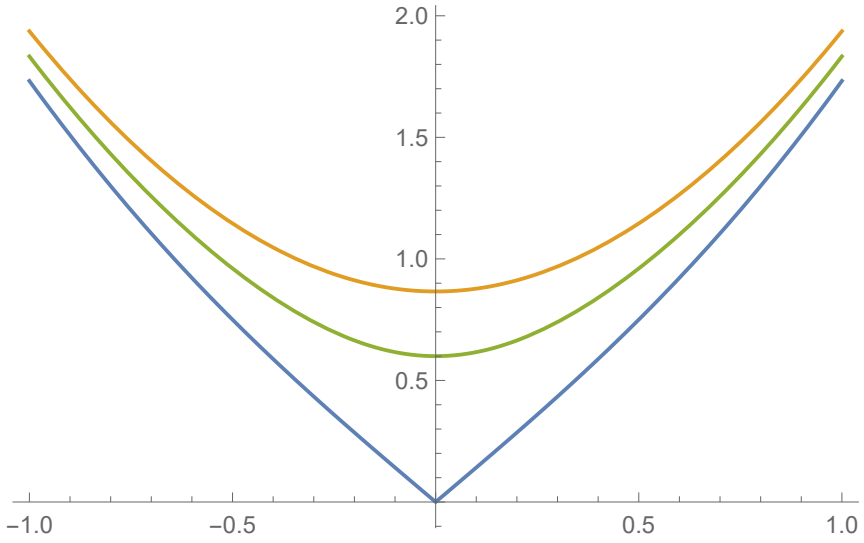

Figure 3.1: Dispersion relation of eq. (3.17) for $\mu = 1$ and $\lambda = 0.25$ (orange),$\lambda = 0.40$ (green) and at the critical point $\lambda_{crit} = 0.50$ (blue). We can see that at the critical point the gap closes.

which for big p goes as $\langle \psi_p^\dagger \psi_p \rangle \propto \frac{1}{p^4}$. Thus, the density in real space is not UV diverging in $d \leq 3$.

In theories where the Hamiltonian includes terms with up to two creation/annihilation operators the two point function is sufficient to describe the state. As seen in section 2.2 the correlation functions in momentum space $\langle \psi_p^\dagger \psi_p \rangle_D$ are given as polynomials of the form $\frac{A}{(p^2+B)^n}$ with $n = 1, 2 \ldots 2D$. We want to expand the exact correlation function in powers of p, such that we can compare with our GCTNS results and compare up to which point our approximate function could in pronciple coincide with the exact one.

The correlation function from eq.(3.19) can be written as

$$\langle \psi_p^\dagger \psi_p \rangle = \frac{1}{2} \left(\frac{1}{\sqrt{1 - \frac{4\lambda^2}{(p^2+\mu)^2}}} - 1 \right)$$

We set $x = \frac{4\lambda^2}{(p^2+\mu)^2}$ and use the expansion

$$(1-x)^a = \sum_n^\infty \binom{a}{n} x^n \tag{3.20}$$

Thus, we obtain

$$\langle \psi_p^\dagger \psi_p \rangle = \frac{1}{2} \left(\frac{1}{2} \frac{4\lambda^2}{(p^2+\mu)^2} + \frac{3}{8} \left(\frac{4\lambda^2}{(p^2+\mu)^2} \right)^2 + \frac{5}{16} \left(\frac{4\lambda^2}{(p^2+\mu)^2} \right)^3 + \frac{35}{128} \left(\frac{4\lambda^2}{(p^2+\mu)^2} \right)^4 + \mathcal{O}\left(\frac{4\lambda^2}{(p^2+\mu)^2} \right)^5 \right)$$

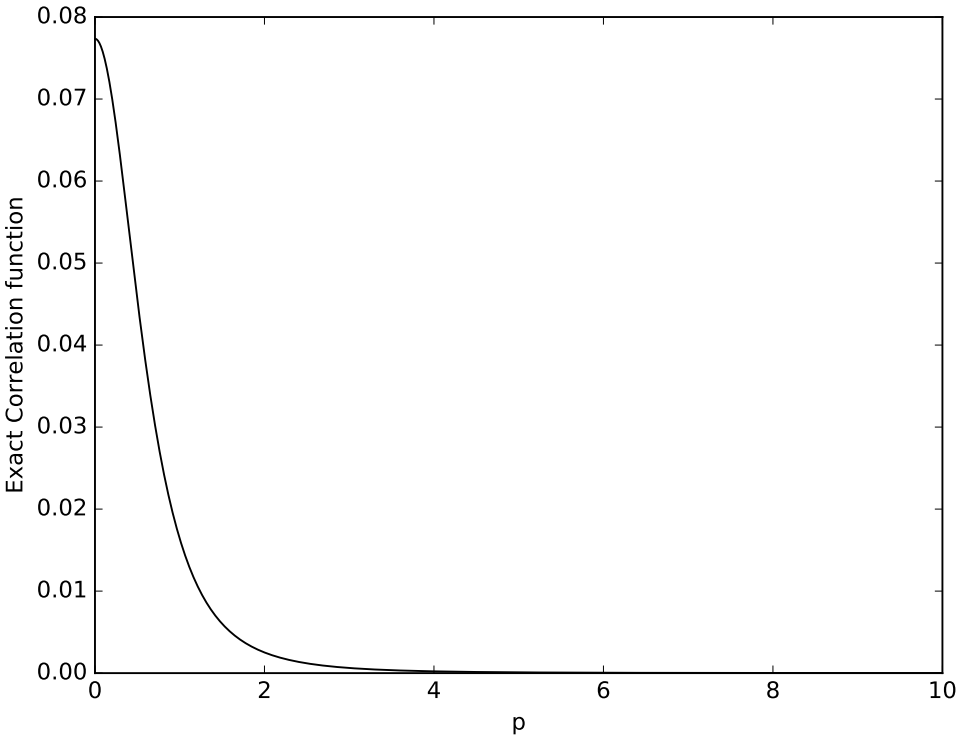

Figure 3.2: The correlation function in momentum space $\langle \psi_p^\dagger \psi_p \rangle$ for $\mu = 1$ and $\lambda = 0.25$.

to

(3.22)

The series converges for $\frac{4\lambda^2}{(p^2+\mu)^2} \leq 1$, thus in the non-critical regime. The series is not converging anymore when the energy gap closes, so at the critical point.

Far from the critical point, for $4\lambda^2 \ll (p^2+\mu)^2$, the leading term of the correlation function is

$$\langle \psi_p^\dagger \psi_p \rangle = \frac{\lambda^2}{(p^2+\mu)^2}.$$

The bigger λ gets, the smaller the energy gap, the more terms in the expansion become relevant. Only these terms will contribute to the numerical result, so only they will be approximated.

3.4 GCTNS in 1d

Now that we understand the model and its exact analytic solution we will use the GCTNS method to solve the problem variationally. As the Hamiltonian is quadratic in the creation and annihilation operators, the correlation function describes the system as well as the energy does. Thus, we could approximate either of those quantities by our variational state.

In this report we did everything by optimizing w.r.t the energy, as for later generalizations to different hamiltonians it is more helpful.

The first step in order to apply the variational method is to express the energy density as the expectation value of our given Hamiltonian density

$$E = \langle V, a|h(x)|V, a\rangle = \langle \frac{\partial\psi^\dagger(x)}{\partial x}\frac{\partial\psi(x)}{\partial x}\rangle + \mu\langle\psi^\dagger(x)\psi(x)\rangle + \lambda\left(\langle\psi^\dagger(x)\psi^\dagger(x)\rangle + \langle\psi(x)\psi(x)\rangle\right) \tag{3.23}$$

where we can compute the summands with the tools we developed in 2.2. We can start from some general Gaussian state

$$|V, a\rangle = \int D\phi \exp\left\{\int d^dx(-\frac{1}{2})\phi(x)(-\nabla^2 + V)\phi(x) + a\phi(x)\psi^\dagger(x)\right\}|0\rangle,$$

with some initial energy $E_{init} > E_0$. One can show that we can always transform the $\phi(x)$ vector by a unitary transformation, such that V is diagonal. Starting with some generic diagonal, complex V matrix and some complex a vector one can iteratively change this parameters in the variational method algorithm, given by eq.(2.2) and evolve towards states with lower energy. The ingredients to compute the descent are given in sections 2.3.1 and 2.3.2.

Now we perform a brief check of how well our GCTNS method works. We choose $\mu = 1$ and $\lambda = 0.25$. In this regime we are far from the critical point. In Fig. 3.3 the evolution of the energy density and in Fig. 3.4 and the evolution of the parameters is shown. It is done for the simple case where $D = 2$ and we get $E_0 = -0.03205936$. To benchmark our result we compute the lowest energy value exactly. Having the energy density in momentum space (3.16) one can compute the energy density in real space for a translational invariant system

$$\varepsilon_0 = \frac{1}{L}\sum_{-\infty}^{+\infty}\epsilon_0(p) = \frac{1}{\pi}\int_0^{+\infty}\epsilon_0(p)dp. \tag{3.24}$$

The integral is convergent and for $\mu = 1$ and $\lambda = 0.25$ we get $\varepsilon_0 = -0.03205936$. Already for such a low bond dimension we see that the results of the GCTNS are very good, we have a relative error of $\frac{|\varepsilon_0 - E_0|}{\varepsilon_0} = 1.4 \cdot 10^{-9}$. For higher bond dimension one expects the results to improve. However, here the precision is already very good in $D = 2$.

Now we apply the same method to the case where $\mu = 1$ and $\lambda = 0.49$ so we are close to the critical point, which means that the energy gap from eq.(3.17) is about to close, i.e. $\Delta E \to 0$. The algorithm is still stable. We expect the approximation to be worse, than far away from the critical point, see sections 1.1.2 and 3.4.1. The analytical value of the ground state energy density now is $\varepsilon_0 = -0.1406884304$, whereas the value we get with the GCTNS method for D=2 is $E_0 = -0.1406846799$. Now the relative error is clearly bigger, namely $\frac{|\varepsilon_0 - E_0|}{\varepsilon_0} = 5.3 \cdot 10^{-4}$. It is necessary to go to higher bond dimensions in order to achieve higher precision. In Fig. 3.5 one can see that as we increase the bond dimension the actual lowest energy value is approximated better.

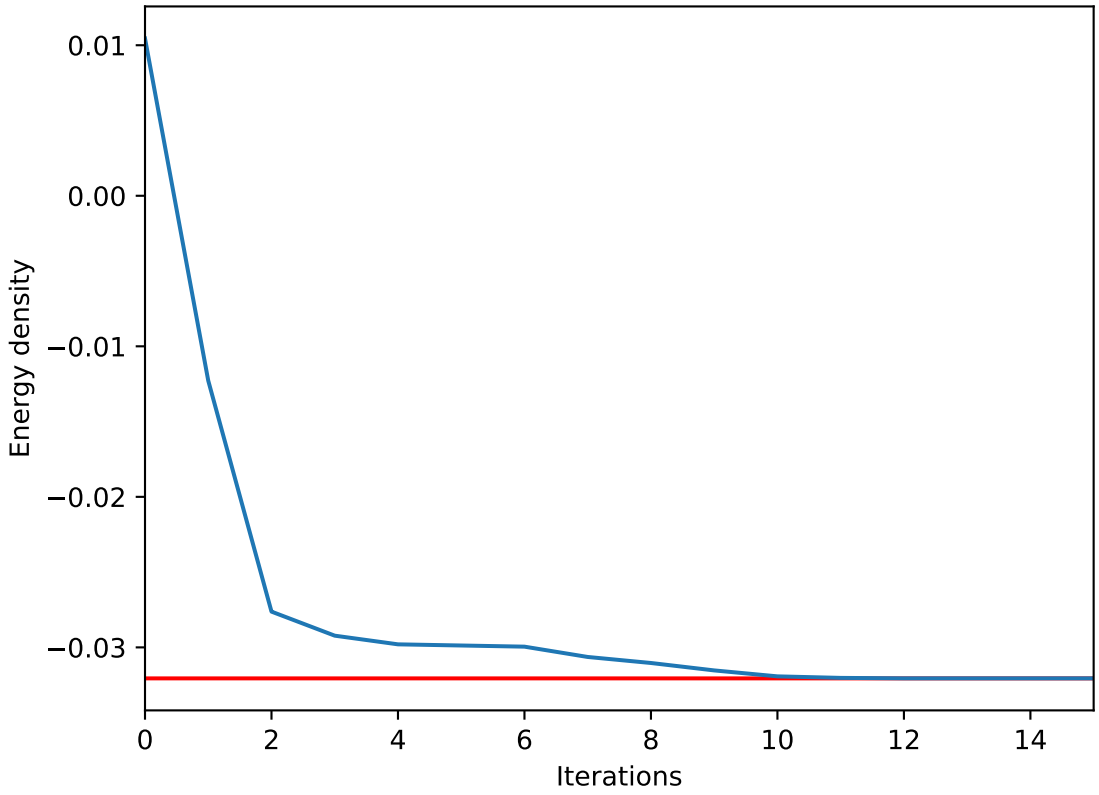

Figure 3.3: Energy descent in d=1 for bond dimension D=2(blue) and the exact ground energy density value $\varepsilon_0 = -0.03205936$ (red). The lowest energy density value we get is $E_0 = -0.032059364$. We have a relative error of $\frac{|\varepsilon_0 - E_0|}{\varepsilon_0} = 1.4 \cdot 10^{-9}$.

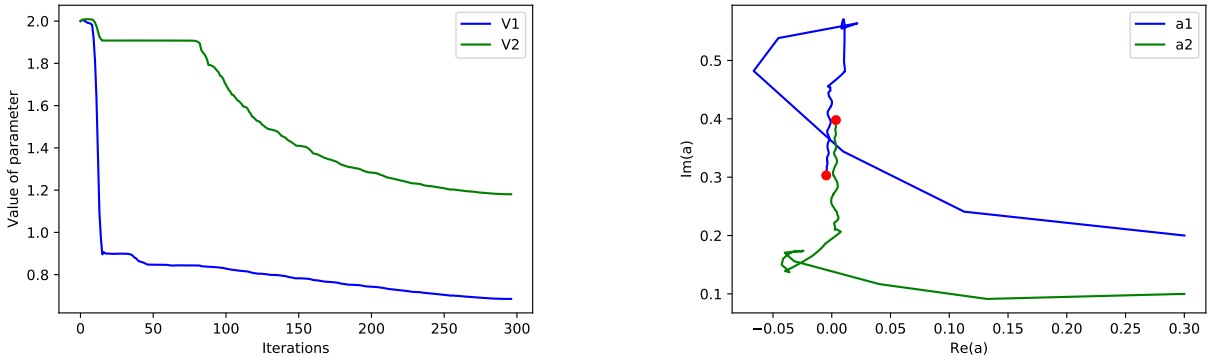

(a) Evolution of V

(b) Evolution of a

Figure 3.4: The evolution of the parameters V_{11}(blue) and V_{22}(green) on the left, and of the parameters a_1(blue) and a_2(green) on the right. Here $d = 1$, $D = 2$, $\mu = 1$ and $\lambda = 0.25$.

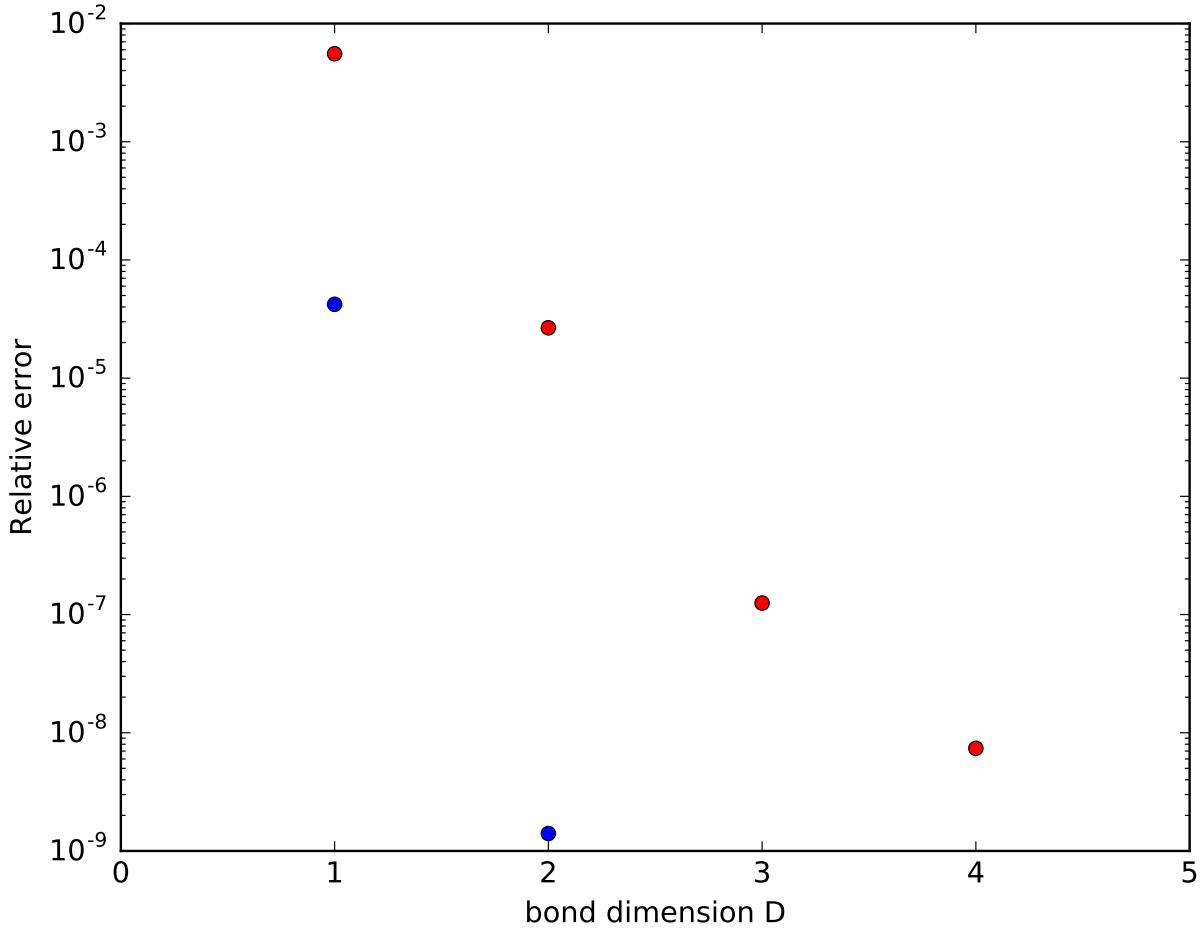

Figure 3.5: Dependence of the relative error of the ground state energy $\frac{|\varepsilon_0 - E_0|}{\varepsilon_0}$ on the bond dimension D, in the case where $\lambda = 0.25$ (blue) and $\lambda = 0.49$ (red). The approximation is much better for the non critical case.

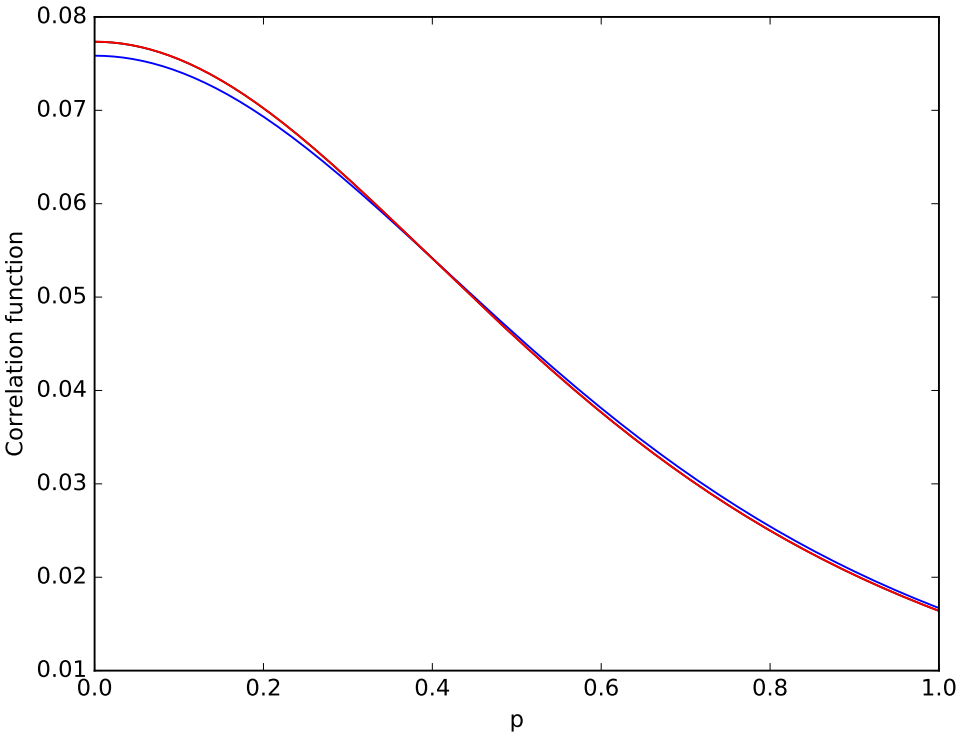

(a) For $\lambda = 0.25$ and $\mu = 1$

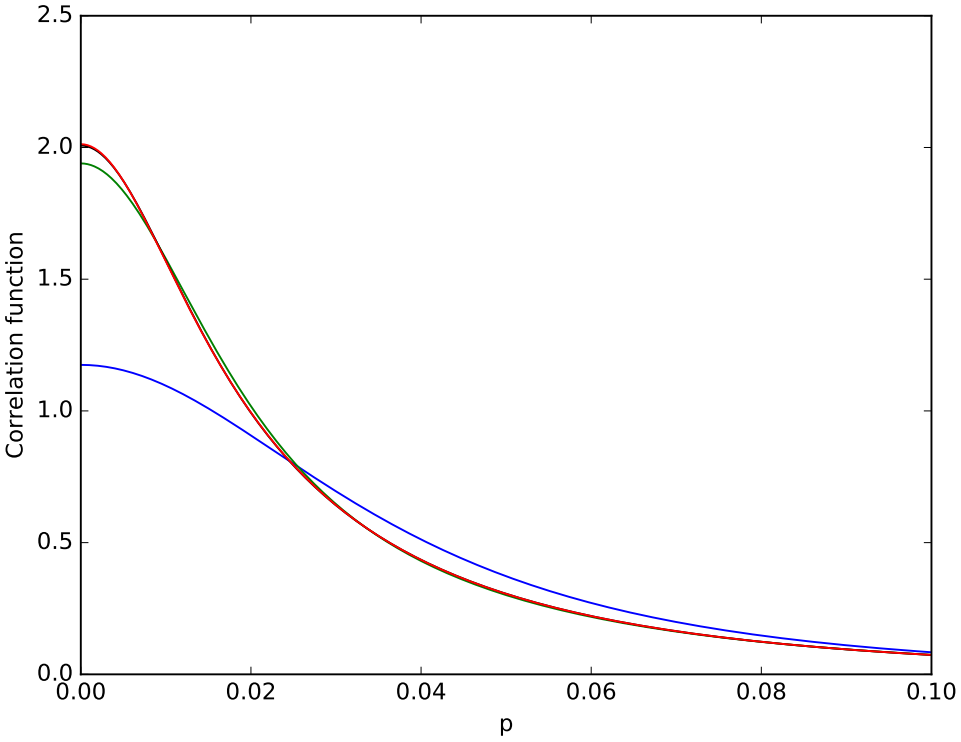

(b) For $\lambda = 0.49$ and $\mu = 1$.

Figure 3.6: The correlation function in momentum space is plotted for $D = 1$ (blue), $D = 2$ (green), $D = 3$ (black) and the exact value (red). The lines which are not visible overlap with the exact function.

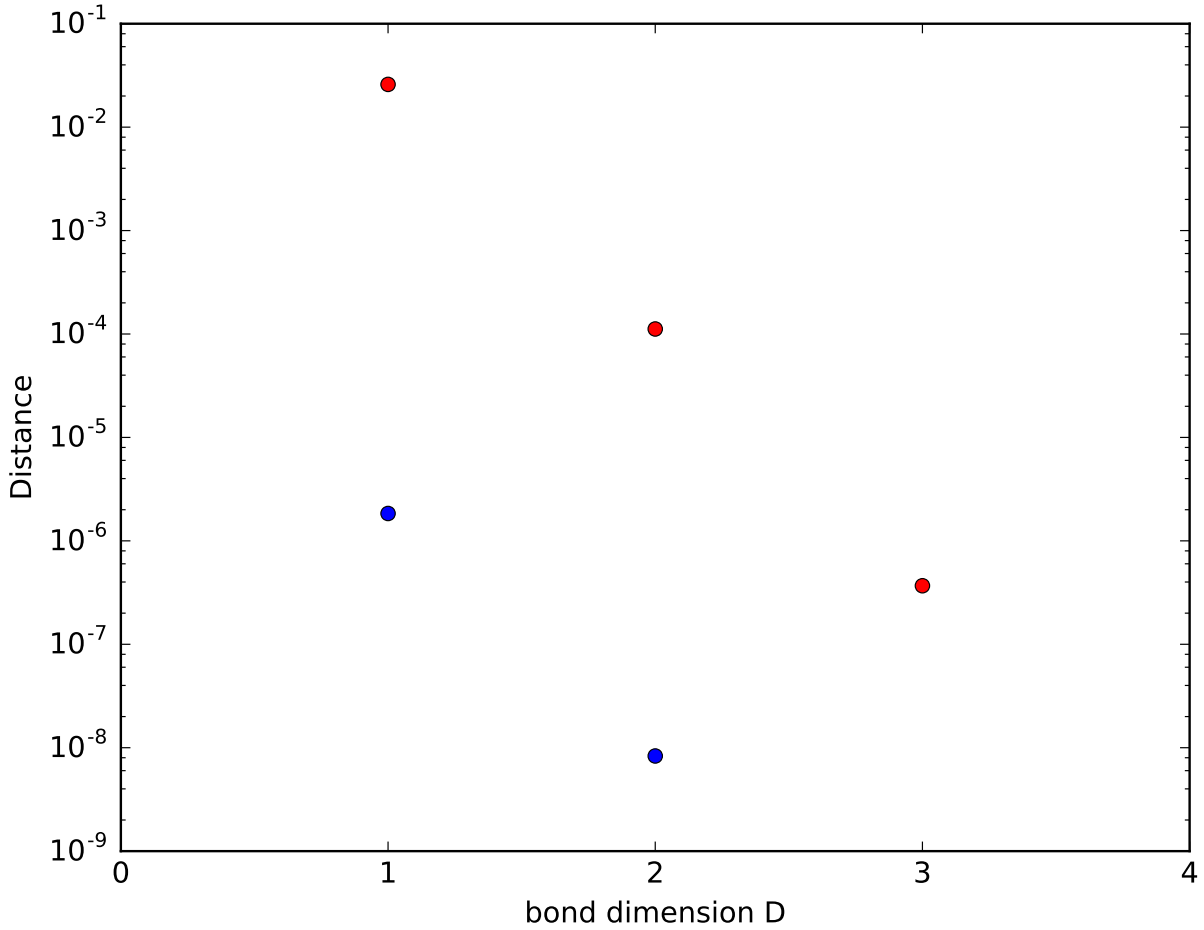

Figure 3.7: Here the relative distance $\sqrt{\frac{\int dp|\langle\psi_p^\dagger\psi_p\rangle_{D=2}-\langle\psi_p^\dagger\psi_p\rangle|^2}{\int dp|\langle\psi_p^\dagger\psi_p\rangle|^2}}$ between the exact and the variational correlation function $\langle\psi_p^\dagger\psi_p\rangle_{D=2}$ is plotted, as a function of the bond dimension. Far from the critical point with $\mu = 1$ and $\lambda = 0.25$ (blue) and close to it with $\mu = 1$ and $\lambda = 0.49$ (red). The approximation is much better far away from the critical point.

3.4.1 Comparison of correlation functions

In our model a two point correlation function is also sufficient to describe a state. Even though we approximate with respect to the energy, we will see that the correlation function also gets approximated simultaneously. The reason is that these two methods, for a quadratic Hamiltonian, are equivalent. In this subsection we will see how the GCTNS correlation function is approximating the exact one and gain some intuition.

Lets suppose we run the program for $D = 1$, the simplest case. We can compute the exact form of the correlation functions

$$\langle \psi_p^\dagger \psi_p \rangle_{D=1} = \frac{|a|^4}{|p^2 + V|^2 - |a|^4} \tag{3.25}$$

where V and a are now simply numbers. The analytic correlation function is given by (3.21). If we take μ and λ such that we are not at the critical point, we know that the correlation function is very well approximated by the first terms of the expansion,

$$\langle \psi_p^\dagger \psi_p \rangle = \frac{\lambda^2}{(p^2+\mu)^2} + 3\left(\frac{\lambda^2}{(p^2+\mu)^2}\right)^2 + \mathcal{O}\left(\frac{\lambda^2}{(p^2+\mu)^2}^2\right). \tag{3.26}$$

The program optimizes V and a, such that the energy is minimal. This is equivallent to pushing the algorithm to minimize the numerical difference between (3.25) and (3.26).

For example, after running the program for $\lambda = 0.1$ and $\mu = 1$ we arrive at $|a|^2 = 0.0998 \simeq \lambda$ and $|V| = 0.98 \simeq \mu$, thus

$$\frac{|a|^4}{|p^2 + V|^2 - |a|^4} \simeq \frac{\lambda^2}{(p^2+\mu)^2}$$

As λ gets larger the second term of the expansion starts getting more important. Now the program still tries to fix the parameters such that it compensates for the additional contribution. The approximation is worse, as the $\langle \psi_p^\dagger \psi_p \rangle_{D=1}$ function lacks terms with a p^{-4} dependence. If we would go to higher bond dimensions, $D = 2$ we would have this dependence, so we could again find the exact solution, where (3.26) coincides with the $\langle \psi_p^\dagger \psi_p \rangle_{D=2}$. In Fig.3.6b it becomes clear that for $\mu = 1$ and $\lambda = 0.25$ choosing $D = 2$ is already sufficient. The closer we get to the critical point the more terms of the correlation expansion become relevant and the higher we have to go in D.

The smaller the bond dimension the less parameters the program needs to optimize, but we loose in precision. The fact that the variational method is that efficient already in so low bond dimensions makes it a very promising tool, as it has one main advantage, compared to the analytic solution: It could be used in principle also for non integrable models.

3.5 GCTNS in 2 dimensions

When implementing exactly the same gradient descent method to GCTNS in 2 spacial dimensions one encounters one main problem. The energy descent never converges, in

contrast to what we had seen in the 1 dimensional case in Fig. 3.3. The energy keeps on decreasing and with it the values of the parameters keep on alternating. To understand this behaviour we look at the exact analytic results. The energy density in real space

$$\varepsilon_0 = \frac{1}{4\pi^2}\int_{-\infty}^{+\infty}\frac{1}{2}\left(\sqrt{(p^2+\mu)^2-4\lambda^2}-(p^2+\mu)\right)d^2p$$

is diverging to $-\infty$. Looking at the expansion of the integrand

$$\epsilon_0(p) = -\frac{\lambda^2}{(p^2+\mu)} - \frac{\lambda^4}{(p^2+\mu)^3} + \mathcal{O}\left(\left(\frac{4\lambda^2}{(p^2+\mu)^2}\right)^5\right).$$

we see that integrating over p in $d=2$ the first term is diverging logarithmically. Note that in one dimension this was not the case.

Thus, the program is trying to approximate a state of infinite negative energy. This does not mean necessarily that there is no ground state, but it definately means that we cannot compare our GCTNS results with the analytic ones and that the programm will never stop running.

We could change the algorithm and optimize the parameters with respect to the correlation function. In the case of a quadratic Hamiltonian, the two point function contains all the relevant physical information of the state. Thus, approximating the two point function is the same as approximating the lowest energy. For more generic Hamiltonian with higher order terms, the two point function is not enough to describe the state, we also need higher order moments. Thus, in the more generic case one is forced to proceed by minimizing the energy. In order to have a more generic tool, we will still optimize with respect to the energy density. Therefore we need to find a way to circumvent the problem differently.

To proceed we need to gain some more insight in the form of divergencies of the GCTNS energy E_0.

3.5.1 Divergent terms of the GCTNS

When we compute the energy for the GCTNS

$$E = \langle V,a|h(x)|V,a\rangle = \langle\frac{\partial\psi^\dagger(x)}{\partial x}\frac{\partial\psi(x)}{\partial x}\rangle + \mu\langle\psi^\dagger(x)\psi(x)\rangle + \lambda\left(\langle\psi^\dagger(x)\psi^\dagger(x)\rangle + \langle\psi(x)\psi(x)\rangle\right) \tag{3.27}$$

we realize that some of the terms diverge in 2 dimensions, other than in 1 dimension. For example the closed formula for the last term is computed in 2.2

$$\langle\psi^\dagger(x)\psi^\dagger(x)\rangle = \sum_i^{2D}(\mathbf{a}^{*T}\cdot U)_i(U^{-1}\cdot\mathbf{a}^*)_i\int_0^\Lambda\frac{d^dp}{(2\pi)^d}\frac{1}{p^2+\lambda_i} \tag{3.28}$$

$$= \frac{1}{4\pi}\sum_i^{2D}(\mathbf{a}^{*T}\cdot U)_i(U^{-1}\cdot\mathbf{a}^*)_i[\log(\Lambda^2+\lambda_i) - \frac{1}{4\pi}\log(\lambda_i)] \tag{3.29}$$

where we introduced a cutoff, as the integral $\int_0^\infty \frac{d^d p}{(2\pi)^d} \frac{1}{p^2+\lambda_i}$ is diverging. Similarly, the terms $\langle \psi^\dagger(x)\psi^\dagger(x)\rangle$ and $\partial^2\langle \psi^\dagger(x)\psi(x)\rangle$ also contain divergent parts. We now investigate this divergent terms and quantify their divergence.

$$\begin{aligned}\partial^2\langle \psi^\dagger(x)\psi(x)\rangle &= \log\Lambda^2[a_1^2+a_2^2+...+a_D^2][a_1^{*2}+a_2^{*2}+...+a_D^{*2}] + \text{finite} \\ &= \log\Lambda^2 \sum_{i=1}^{D} \left((Re[a_i])^2-(Im[a_i])^2\right)^2 + (2Re[a_i]Im[a_i])^2 + \text{finite} \end{aligned} \tag{3.30}$$

and

$$\langle \psi^\dagger(x)\psi^\dagger(x)\rangle + \langle \psi(x)\psi(x)\rangle = 2\log\Lambda^2 \sum_{i=1}^{D} (Re[a_i])^2-(Im[a_i])^2 + \text{finite}\,. \tag{3.31}$$

Thus, the divergent part of the energy is

$$\begin{aligned} f_\infty(a) = \log\Lambda^2 \sum_{i=1}^{D} \left((Re[a_i])^2-(Im[a_i])^2\right)^2 + (2Re[a_i]Im[a_i])^2 \\ +2\lambda\left[(Re[a_i])^2-(Im[a_i])^2\right] \end{aligned} \tag{3.32}$$

We want to find the condition under which the divergent part is maximal, as it would correspond to the lowest energy. Imposing $\frac{f(a)}{\partial Re[a_1]} = 0$ and $\frac{f(a)}{\partial Im[a_1]} = 0$ we arrive at the conditions

$$\sum_{i=1}^{D} Rea_i Ima_i = 0 \tag{3.33}$$

and

$$\sum_{i=1}^{D} (Re[a_i])^2-(Im[a_i])^2 = -\lambda \tag{3.34}$$

So two of the parameters are dependent. These constraints keep the state in a manifold $\mathcal{A}$ where the energy is diverging maximally.

To get a better insight of what exactly is happening in this submanifold of states we investigate in the case of bond dimension $D = 1$. The constraints take the simple form

$$Rea \cdot Ima = 0 \tag{3.35}$$

$$(Re[a])^2-(Im[a])^2 = -\lambda \tag{3.36}$$

so

$$a^2 = -\lambda, \tag{3.37}$$

with $a \in \mathbb{R}$ or $a \in \mathbb{I}$.

The exact form of the correlation function in that case is

$$\langle \psi_p^\dagger \psi_p\rangle_{D=1} = \frac{|a|^4}{|p^2+V|^2-|a|^4} \to \frac{\lambda^2}{|p^2+V|^2-\lambda^2} \tag{3.38}$$

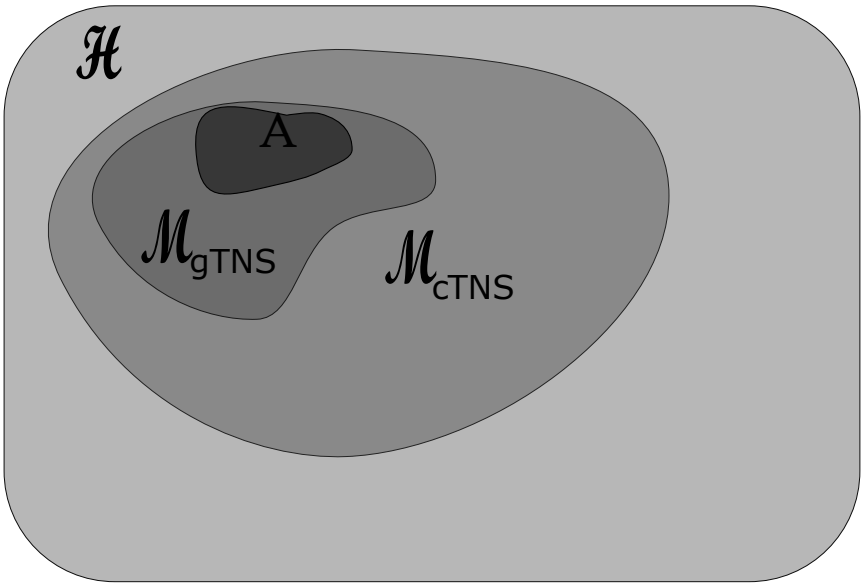

Figure 3.8: $\mathcal{A} \in \mathcal{M}_{GCTNS} \in \mathcal{M}_{cTNS} \in \mathcal{H}$.

We see that it is very close to the form of the exact correlation function $\frac{\lambda^2}{(p^2+m)^2}$. Thus, being in that manifold allows us to still approximate the state well enough, for $V \simeq \mu$. Now only one parameter is free.

On the other hand one can look at the form of the energy

$$\begin{aligned} E_0(p) &= \partial^2 \langle \psi_p^\dagger \psi_p \rangle + \mu \langle \psi_p^\dagger \psi_p \rangle + \lambda \left(\langle \psi_p^\dagger \psi_{-p}^\dagger \rangle + \langle \psi_p \psi_{-p} \rangle \right) \\ &= -\frac{\lambda^2}{|p^2+V|^2 - \lambda^2}(p^2+\mu) + \frac{\lambda^2(2\mu - V + V^*)}{|p^2+V|^2-\lambda^2} \end{aligned} \tag{3.39}$$

As we realized in the case of the correlation function the program will optimize around $V \simeq \mu$ such that

$$E_0(p) \simeq -\frac{\lambda^2}{(p^2+\mu)} \tag{3.40}$$

which corresponds to the first term of the energy expansion, eq. (3.16).

In higher D again the constraints will fix the state at a point were the energy will diverge logarithmically. At this point, it is important to notice, that the variational class of GCTNS seems to be so good, that it can even capture the divergence of the actual ground state.

3.5.2 Variational Method on non-divergent terms

It is obvious that to find the lowest energy one has to first maximize the term with the biggest (negative) contribution. That is why we chose parameters which maximize the diverging part of the tensor network energy. Being in this submanifold of states we ensure

that the diverging term is maximal. We found the elements of the submanifold analytically, though one could also use numerical techniques. After being in the correct manifold we apply the same techniques as we did in 1 dimension, namely we optimize the parameters with a variational method.

The energy can be splitted in the finite and the infinite part

$$E = E^R + E^\infty \tag{3.41}$$

So when computing E^R with the GCTNS method, we keep only the finite parts of the relations $\langle \frac{\partial\psi^\dagger(x)}{\partial x}\frac{\partial\psi(x)}{\partial x}\rangle$, $\langle\psi^\dagger(x)\psi(x)\rangle$, $\langle\psi^\dagger(x)\psi^\dagger(x)\rangle$ and $\langle\psi(x)\psi(x)\rangle$. Again we optimize the paramteres such that we get the mimimal E_0^R.

We can actually compare this with the finite part of the exact energy. We define $\epsilon^R(p)$ nondiverging/renormalized part of the energy as

$$\epsilon_0^R(p) = \epsilon_0(p) + \frac{\lambda^2}{(p^2+\mu)} \tag{3.42}$$

which we can integrate and get an exact value. For example for $\mu = 1$ and $\lambda = 0.25$ we get

$$\varepsilon_0^R = \int \frac{d^2p}{(2\pi)^2}\epsilon_0^R = -0.00016630736 \tag{3.43}$$

The program tries to approximate this ε_0^R energy. It optimizes the parameters in the submanifold such that E^R is minimal. We get $E_0^R = -0.00016565273$ with a relative error of $\frac{E_0^R-\varepsilon_0^R}{\varepsilon_0^R} = 0.0039$. It can be improved if we take higher bond dimensions, in analogy with the 1 dimensional case.

When looking at the resulting correlation function, Fig.3.9 and comparing it to the exact correlation function from eq. (3.19), one can see that our tensor network approximation is very good already for $D = 2$. The differernce between the exact and approximate two point function is $\sqrt{\frac{\int d^2p|\langle\psi_p^\dagger\psi_p\rangle_{D=2}-\langle\psi_p^\dagger\psi_p\rangle|^2}{\int d^2p|\langle\psi_p^\dagger\psi_p\rangle|^2}} = 1.286128\cdot 10^{-6}$.

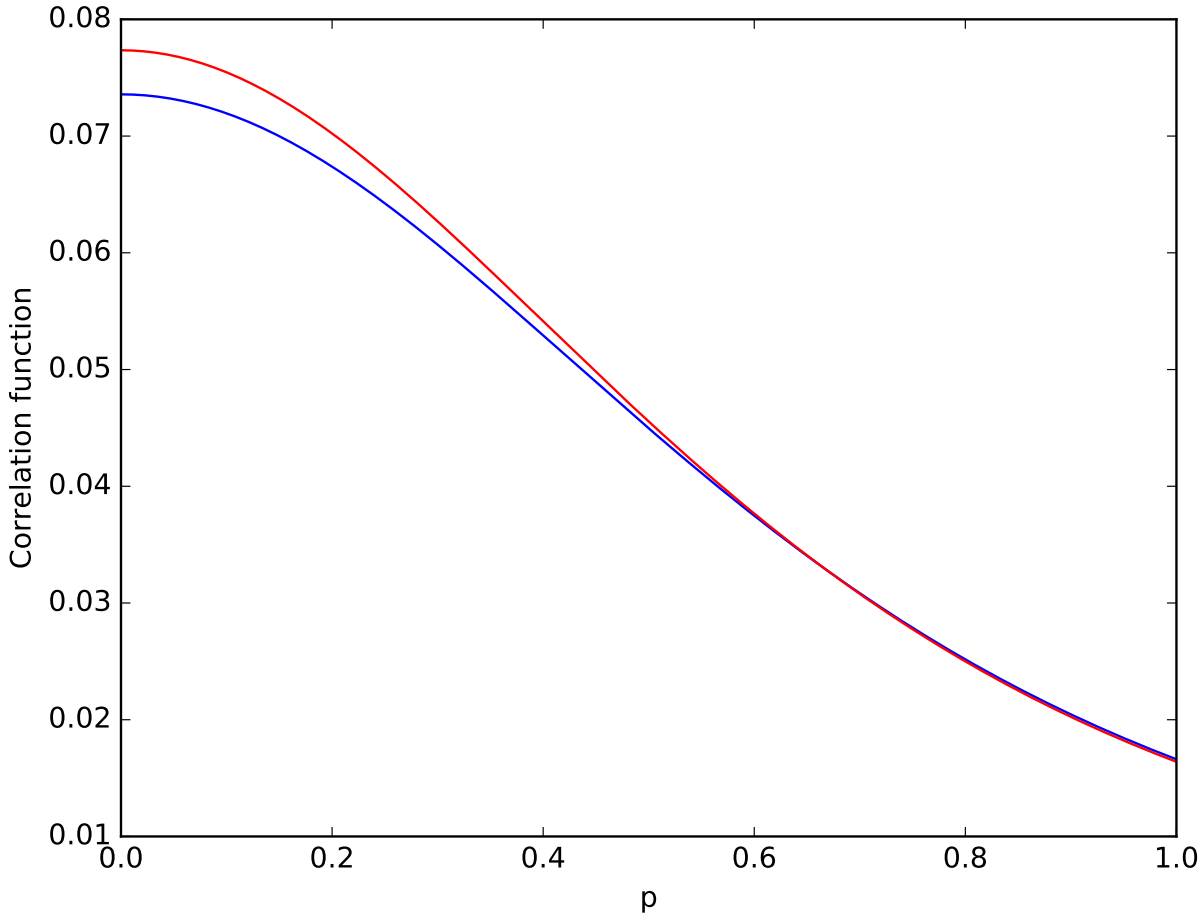

Figure 3.9: In this graph the correlation function in momentum space is plotted. The function we get with the final parameters with GCTNS (green) and the theoretical function (red) overlap, such that they are almost indistinguishable.

Discussion

In this report we tested the variational class of GCTNS on a simple, quasifree model, in one and two dimensions. The results were very satisfying as the approximated ground state was accurate and close to the exact ground state. We were able to see the exponential decay of the correlation functions and approximate these sufficienlty well. Moreover, the GCTNS expectation values inherit exactly the same infinities as the QFT. Thus, they are a good variational Ansatz for ground states of gaussian Hamiltonians in one and two dimensions.

The variational class we used has some main advantages compared to other Ansätze in QFTs. First, it goes beyond the classical solution, in contrast to a simple coherent state. One main property is that the number of parameters is independent of the system size. This makes it a very promising Ansatz for numerical simulations. Moreover, it is defined in arbitrary dimensions, in contrast to the one dimensional cMPS Ansatz. Its efficiency though has not yet been tested in $d > 2$.

To obtain the GCTNS we kept only a very simple form of $V[\psi(x)]$ and $a[\psi(x)]$, see eq. (1.35). One simple generalization is to take $a^{(0)} \neq 0$, which would lead to gaussian states with $\langle\psi_0\rangle \neq 0$, thus breaking the $U(1)$ symmetry of the ground state.

Although we have shown the efficiency of this class of states in a simple model, one could try out different Hamliltonians, which may be non-integrable, such as the Hamiltonian of eq. (3.4), with quartic interactions. In that case the exact ground state is not Gaussian anymore, but still we could find the lowest energy Gaussian approximation. By taking different functions of $V[\psi(x)]$ and $a[\psi(x)]$, with higher order terms, one could create a cTNS which goes beyond Gaussian states. However, computing expectation values in that case is impossible, because of the form of the generating functional (1.30). Therefore one has to keep the GCTNS Ansatz, but could add some perturbation.

The QTNS could also provide a natural continuum version of tensor network toy models of the AdS/CFT correspondence, where scalar field theories on a fixed AdS background are related to conformal field theories on the boundary. One could realize such conditions with GCTNS with the physical field ψ living on the boundary of a two dimensional auxiliary space, populated by the fields ϕ.

Moreover, many interesting questions are so far open. How do V and a encode topological order? Do cTNS generically obey the area law like their discrete counterparts? To what extent does the bond field dimension D quantify entanglement for classes of cTNS? Tackling these questions is an important goal for future work, to fully extend the success of tensor networks from the lattice to the continuum.

Appendices

Appendix A

Appendix: Tensor Network Notation

This is a small overview over the Tensor Network notation and the main Tensor operations. For further understanding, one can read the following literature [5, 1]. Tensors are the generalization of vectors and matrices. A d- dimensional vector can be considered as an element of $\mathbb{C}^d$, and an $n \times m$ dimensional matrix an element of $\mathbb{C}^{n \times m}$. Correspondingly an rank-r tensor of dimensions $d_1 \times d_2 \times ... \times d_r$ is an element of $\mathbb{C}^{d_1 \times d_2 \times ... \times d_r}$. In tensor network notation a single tensor will be represented by a geometric shape with legs sticking out of it, each corresponding to one index, like in these examples of a vector, a matrix and a 3-rank tensor respectively:

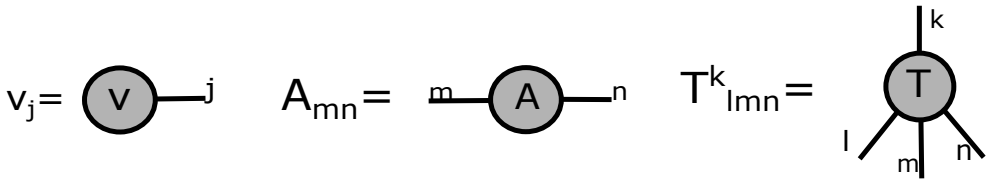

The first operation we will consider is the tensor product, a generalization of the outer product of vectors. The tensor product of $A \in \mathbb{C}^{d_1 \times d_2 \times ... \times d_r}$ and $B \in \mathbb{C}^{d_1 \times d_2 \times ... \times d_n}$ is

$$[A \otimes B]_{i_1,i_2...i_r,j_1,j_2,...j_s} = A_{i_1,i_2...i_r} \cdot B_{j_1,j_2,...j_s} \in (\mathbb{C}^{d_1 \times ... \times d_r} \otimes \mathbb{C}^{d_1 \times ... \times d_n}) \tag{A.1}$$

and is represented as

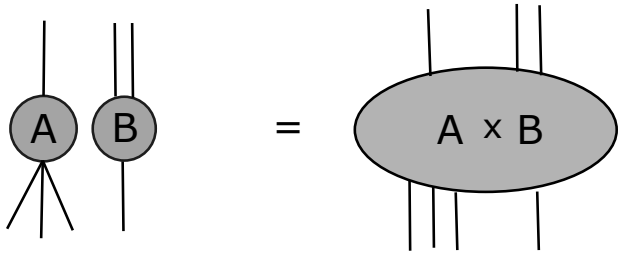

Given a tensor A, for which the xth and yth indices have identical dimensions ($d_x = d_y$), the partial trace over these two dimensions is simply a joint summation over that index

$$[Tr_{x,y}A]_{i_1,i_2...i_{x-1},i_{x+1},..,i_{y-1},i_{y+1}...i_r} = \sum_{a}^{d_x} A_{i_1,i_2...i_{x-1},a,i_{x+1},..,i_{y-1},a,i_{y+1}...i_r}, \tag{A.2}$$

and is represented as

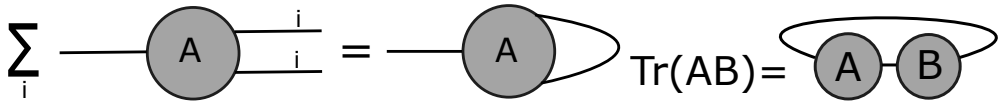

An essential tensor operation for tensor networks is the tensor contraction, corresponding to a tensor product followed by a trace between indices of the two tensors,

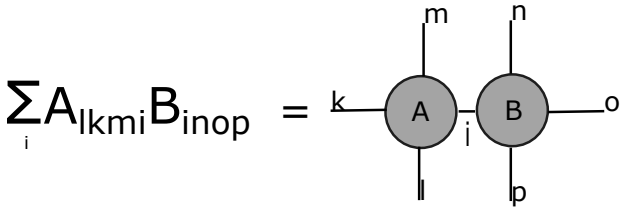

A.1 Singular Value Decomposition (SVD)

A key mathematical ingredient in numerical algorithms when dealing with Tensor Networks is the Singular Value Decomposition (SVD), a factorization of a real or complex matrix. Suppose A is an $m \times n$ matrix whose entries come from the field K, which is either the field of real numbers or the field of complex numbers. Then the singular value decomposition of A exists, and is a factorization of the form:

$$A = U\Sigma V^{\dagger} \tag{A.3}$$

where U is a $m \times m$ unitary matrix, V is a $n \times n$ unitary matrix, Σ a $m \times n$ diagonal matrix, which entries are called singular values. A common convention is to list the singular values in descending order. In this case, the diagonal matrix Σ is uniquely determined by A.

An operation which is often used when working with tensor networks is a **truncated SVD**. In this case only the D column vectors of U and D row vectors of $V^{\dagger}$ corresponding to the D largest singular values Σ are calculated. The rest of the matrix is discarded, such that

$$\tilde{A} = U_D \Sigma_D V_D^{\dagger} \tag{A.4}$$

This can be much quicker and more economical than computing the exact SVD. The matrix U_D is thus $m \times D$, Σ_D is $D \times D$ diagonal, and $V_D^{\dagger}$ is $D \times n$. Of course the truncated

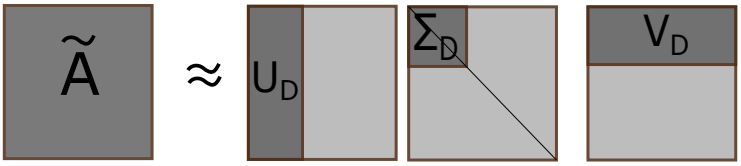

Figure A.1: Reconstruction of the matrix from a small number of singular values, truncated SVD

SVD is no longer an exact decomposition of the original matrix A, but the approximate matrix $\tilde{A}$ is in a very useful sense the closest approximation to A that can be achieved by a matrix of rank D.

A.2 Tensor Networks

A Tensor Network is a diagram which tells us how to combine several tensors into a single composite tensor. The rank of this overall tensor is given by the number of unmatched tensor legs. Tensor networks can be contracted by beginning with a single tensor and

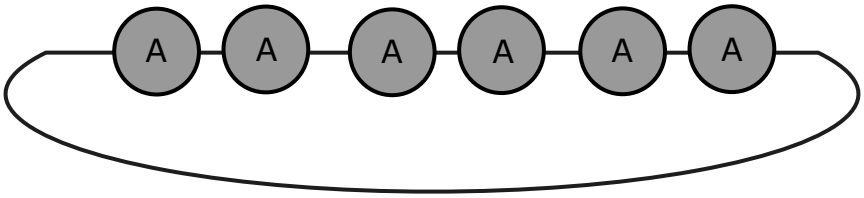

(a) A zero rank tensor, just a number.

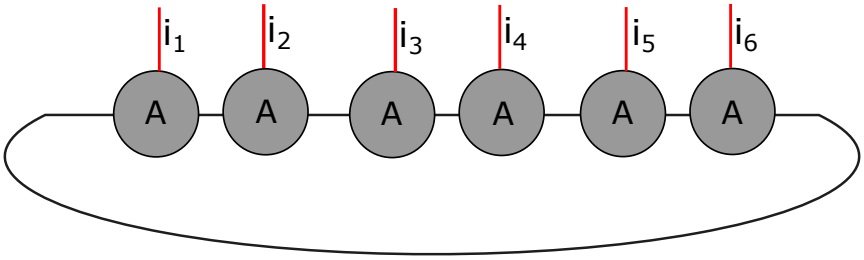

(b) 6 rank tensor

Figure A.2: Examples of 1 dimensional Tensor networks. From the diagram one can read how to contract the matrices(a) or tensors(b).

repeatedly contracting it against tensors one at a time. For example the composite tensor of Fig.A.3b can be computed iteratively by contracting more and more tensors together, as seen in Fig. A.4. It is important to note that the form/rank of the tensors in $d \geq 2$ changes, while in $d = 1$ it stays the same. By applying this grouping iteratively we can compute the final overall tensor.

While in the simple 1 dimensional case this is trivial, in 2 dimensions it is not. First, there are different lattice structures, as triangular lattices, tree-like and MERA structures [14]. Furthermore, one can notice that there are computationally cheaper ways to compute the final tensor. Many different methods of contracting the tensors have been developed over the years, as boundary MPS [30], corner transfer matrices [31] and Tensor coarse graining [32]. In the latter we group neighboring tensors into new, higher rank tensors, see Fig.A.5.

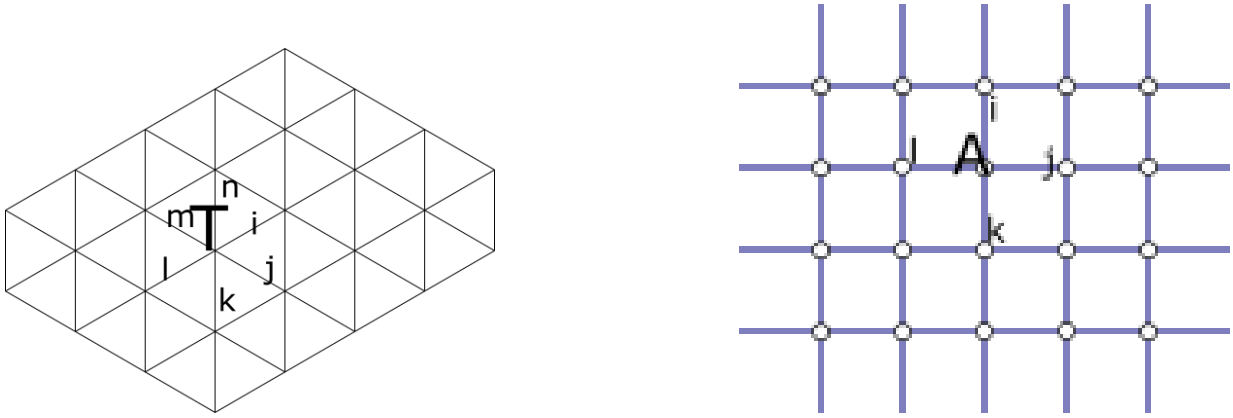

(a) Triangular Lattice. (b) Square Lattice

Figure A.3: Examples of Tensor Networks in $d = 2$.

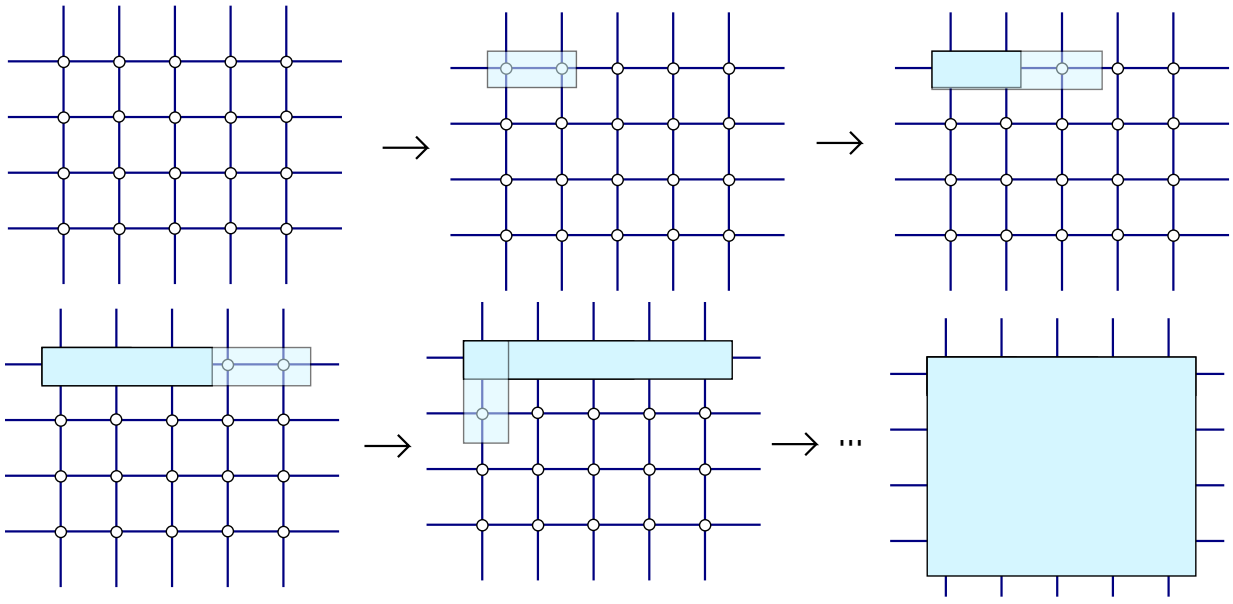

Figure A.4: Naive contraction of tensors to obtain overall tensor. After every contraction the rank of the tensor gets bigger

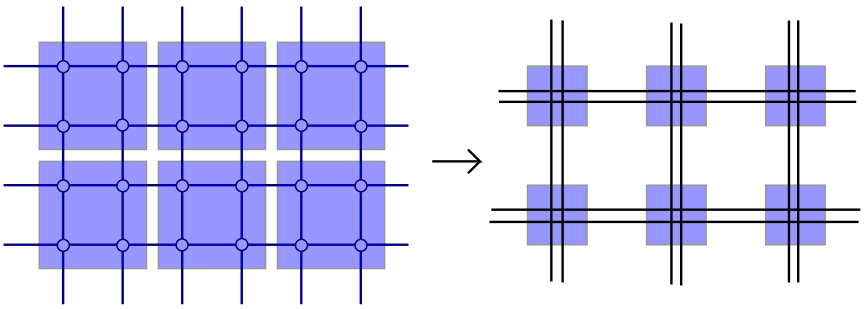

Figure A.5: Grouping tensors into new, higher rank tensors. Here the initial tensors were 4 rank, the resulting ones are 8 rank.

Appendix B

Appendix: Path integral formulation

We can reformulate the cMPS state so that expectation values for the auxiliary system are expressed as path integrals [23]. The motivation is to expand the cMPS to higher dimensions, respecting the symmetries of the physical state in terms of symmetries of an action for the auxiliary system. We will explain only the similarity between a tensor contraction and a path integral over an auxiliary field in the simple case of a cMPS.

We start by writing a basis for the auxiliary Hilbert space $\mathcal{H}_{\text{aux}}$ as $|j\rangle_{\text{aux}}$ with $j = 1..., D$. We enlarge the space via second quantization, and introduce bosonic annihilation and creation operators b_j and $b_j^\dagger$ with $[b_j, b_i^\dagger] = \delta_{ij}$. The Hilbert space of the enlarged auxiliary system is that of the Fock space $\mathcal{F}(\mathcal{H}_{\text{aux}})$, which is infinite dimensional. The connection between the two spaces is made by identifying $\mathcal{H}_{\text{aux}}$ with the single particle sector via $|j\rangle_{\text{aux}} = b_j^\dagger|\Omega >_{\text{aux}}$. Now we make the following substitution

$$Q(x) \to Q^{i,j}(x) b_j^\dagger b_i, \tag{B.1}$$

$$R(x) \to R^{i,j}(x) b_j^\dagger b_i \tag{B.2}$$

and obtain the action

$$S(x) = \sum_{i,j} Q^{i,j}(x) b_j^\dagger b_i \otimes \mathbb{1} + R^{i,j}(x) b_j^\dagger b_i \otimes \psi^\dagger(x) \tag{B.3}$$

We divide the space $[0, L]$ in small intervals with uniform spacing ϵ and insert resolutions of the identity

$$\mathbb{1} = \frac{1}{\pi^D} \int \prod_k^D d\phi_k d\phi_k^* |\phi_k\rangle\langle\phi_k| \tag{B.4}$$

where $\phi_k = \exp[\phi_k b_k^\dagger - \phi_k^* b_k]|\Omega >_{\text{aux}}$ is a field coherent bosonic state. Taking the limit where $\epsilon \to 0$ and assuming that only smooth variations of the auxiliary field ϕ contribute, we obtain a path integral

$$|\chi\rangle = \int \mathcal{D}\phi \mathcal{D}\phi^* \exp\{\int_0^L \left(\frac{1}{2}\phi^\dagger(x)\frac{d\phi}{dx}(x) + \frac{d\phi^*}{dx}(x)\phi(x) \right.$$
$$\left. + \phi^\dagger(x)Q(x)\phi(x) + (\phi^\dagger(x)R(x)\phi(x))\psi^\dagger(x)dx\}|\Omega\rangle$$

$$to \tag{B.6}$$

where $\phi = \{\phi_k\}_{k=1}^{D}$ is a vector field. The formulation of the cMPS as a path integral is guiding expression for the generalization to higher dimensional scenarios, which will be described in section 1.3.

Appendix C

Appendix: Integrals

The integrals computed here we need in order to implement the variational code, as we will need to arrive at closed formulas. We only need integrals over momenta in one and two spacial dimensions, as we restrict only to these cases in our example models.

C.1 One dimension

We compute the same integrals in 1 dimension

$$I_1(\lambda_i) = \int \frac{dp}{2\pi} \frac{1}{p^2+\lambda_i} e^{ip(x-y)} = \frac{1}{2\sqrt{\lambda_i}}$$

$$I_{1kin}(\lambda_i) = \int \frac{dp}{2\pi} \frac{p^2}{p^2+\lambda_i} e^{ip(x-y)} = -\frac{\sqrt{\lambda_i}}{2} \tag{C.1}$$

$$I_2(\lambda_i, \lambda_j) = \lim_{x\to y} \int \frac{d^dp}{(2\pi)^d} \frac{1}{p^2+\lambda_i} \frac{1}{p^2+\lambda_j} e^{ip(x-y)} \tag{C.2}$$

for $x \to y$ we get

$$I_2(\lambda_i \neq \lambda_j) = -\frac{1}{2(\sqrt{\lambda_i}+\sqrt{\lambda_j})(\sqrt{\lambda_i}\sqrt{\lambda_j})} \tag{C.3}$$

$$I_2(\lambda_i = \lambda_j) = \frac{1}{4\sqrt{\lambda_i}^3} \tag{C.4}$$

$$I_{2kin}(\lambda_i, \lambda_j) = \lim_{x\to y} \int \frac{d^2p}{(2\pi)^d} \frac{p^2}{p^2+\lambda_i} \frac{1}{p^2+\lambda_j} e^{ip(x-y)} \tag{C.5}$$

for $x \to y$ we get

$$I_{2kin}(\lambda_i \neq \lambda_j) = \frac{1}{2(\sqrt{\lambda_i} + \sqrt{\lambda_j})} \tag{C.6}$$

$$I_{2kin}(\lambda_i = \lambda_j) = \frac{1}{4\sqrt{\lambda_i}} \tag{C.7}$$

for $\Lambda \gg \lambda_i$

$$I_{2kin}(\lambda_i \neq \lambda_j) = \frac{1}{2\pi} \ln \Lambda - \frac{1}{4\pi} \frac{\lambda_i \ln(\lambda_i) - \lambda_j \ln(\lambda_j)}{\lambda_i - \lambda_j} \tag{C.8}$$

$$I_{2kin}(\lambda_i = \lambda_j) = \frac{1}{4\pi} \left[2\log(\Lambda) - 1 - \log(\lambda_i)\right] \tag{C.9}$$

C.2 Two dimensions

We will compute integrals of the form $I_n = \int \frac{d^2p}{(2\pi)^2} C_n(p) e^{ip(x-y)}$. We are interested in the case where $x \to y$, because we use only equal point correlation functions. In our computations we insert a cutoff Λ whenever the integral is divergent, to quantify the divergence. In order to obtain the initial integral one has to take $\Lambda \to \infty$.

$$\begin{aligned} I_1(\lambda_i) &= \int \frac{d^2p}{(2\pi)^2} \frac{1}{p^2 + \lambda_i} e^{ip(x-y)} \\ &= \int_0^{\Lambda^2} \frac{d(p^2)}{4\pi} \frac{1}{p^2 + \lambda_i} \\ &= \frac{1}{4\pi} \log(\Lambda^2 + \lambda_i) - \frac{1}{4\pi} \log(\lambda_i) \end{aligned} \tag{C.10}$$

$$\begin{aligned} I_{1kin}(\lambda_i) &= \int \frac{d^2p}{(2\pi)^2} \frac{p^2}{p^2 + \lambda_i} e^{ip(x-y)} \\ &= \int_0^{\Lambda^2} \frac{dp^2}{4\pi} \frac{p^2}{p^2 + \lambda_i} \\ &= \frac{1}{4\pi} [\Lambda^2 - \lambda_i ln(\Lambda^2 + \lambda_i) + \lambda_i ln(\lambda_i)] \end{aligned} \tag{C.11}$$

$$I_2(\lambda_i, \lambda_j) = \lim_{x \to y} \int \frac{d^dp}{(2\pi)^d} \frac{1}{p^2 + \lambda_i} \frac{1}{p^2 + \lambda_j} e^{ip(x-y)} \tag{C.12}$$

for $x \to y$ we get

$$\begin{aligned} I_2(\lambda_i \neq \lambda_j) &= \int_0^\infty \frac{dp}{2\pi} \frac{p}{(p^2+\lambda_i)(p^2+\lambda_j)} \\ &= \frac{1}{4\pi} \int_0^\infty \frac{dp^2}{(p^2+\lambda_i)(p^2+\lambda_j)} \\ = \frac{1}{4\pi} \int_{\lambda_i}^\infty du \frac{1}{u \cdot (u-\lambda_i+\lambda_j)}, u &= p^2+\lambda_i \\ = \frac{1}{4\pi(\lambda_i-\lambda_j)} \int_{\lambda_i}^\infty du [\frac{1}{u} - \frac{1}{u-\lambda_i+\lambda_j}] \\ &= \frac{ln(\lambda_i/\lambda_j)}{4\pi(\lambda_i-\lambda_j)} \end{aligned} \tag{C.13}$$

$$\begin{aligned} I_2(\lambda_i = \lambda_j) &= \frac{1}{4\pi} \int_{\lambda_i}^\infty \frac{d(p^2+\lambda_i)}{(p^2+\lambda_i)^2} \\ &= \frac{1}{4\pi\lambda_i} \end{aligned} \tag{C.14}$$

$$I_{2kin}(\lambda_i, \lambda_j) = \lim_{x \to y} \int \frac{d^2p}{(2\pi)^d} \frac{p^2}{p^2+\lambda_i} \frac{1}{p^2+\lambda_j} e^{ip(x-y)} \tag{C.15}$$

for $x \to y$ we get

$$\begin{aligned} I_{2kin}(\lambda_i \neq \lambda_j) &= \int \frac{d^2p}{(2\pi)^2} \frac{p^2}{p^2+\lambda_i} \frac{1}{p^2+\lambda_j} \\ &= \int_0^{\Lambda^2} \frac{dp^2}{4\pi} \frac{p^2}{p^2+\lambda_i} \frac{1}{p^2+\lambda_j} \\ = \frac{1}{4\pi} \frac{\lambda_i \ln(\lambda_i+\Lambda^2) - \lambda_j \ln(\lambda_j+\Lambda^2)}{\lambda_i-\lambda_j} &- \frac{1}{4\pi} \frac{\lambda_i \ln(\lambda_i) - \lambda_j \ln(\lambda_j)}{\lambda_i-\lambda_j} \end{aligned} \tag{C.16}$$

$$I_{2kin}(\lambda_i = \lambda_j) = \frac{1}{4\pi} \left[\frac{\lambda_i}{\lambda_i+\Lambda^2} + \log(\Lambda^2+\lambda_i) - 1 - \log(\lambda_i) \right] \tag{C.17}$$

for $\Lambda \gg \lambda_i$

$$I_{2kin}(\lambda_i \neq \lambda_j) = \frac{1}{2\pi} \ln \Lambda - \frac{1}{4\pi} \frac{\lambda_i \ln(\lambda_i) - \lambda_j \ln(\lambda_j)}{\lambda_i-\lambda_j} \tag{C.18}$$

$$I_{2kin}(\lambda_i = \lambda_j) = \frac{1}{4\pi} [2\log(\Lambda) - 1 - \log(\lambda_i)] \tag{C.19}$$

$$I_3(V, a, \kappa_i, \kappa_j, \lambda_n) = \int_0^\Lambda \frac{d^2p}{(2\pi)^2} \frac{1}{p^2+\kappa_i} \frac{1}{p^2+\kappa_j} \frac{1}{p^2+\lambda_n} \tag{C.20}$$

For $\kappa_i \neq \kappa_j$ and $\Lambda \gg \lambda_n$

$$I_3(V, a, \kappa_i, \kappa_j, \lambda_n) = -\frac{1}{4\pi} \frac{(\kappa_j - \lambda_n)\ln\kappa_i + (\lambda_n - \kappa_i)\ln\kappa_j + (\kappa_i - \kappa_j)\ln\lambda_n}{(\kappa_j - \lambda_n)(\kappa_i - \lambda_n)(\kappa_i - \kappa_j)}, \tag{C.21}$$

and for $\kappa_i = \kappa_j$ and $\Lambda \gg \lambda_n$

$$I_3(V, a, \kappa_i = \kappa_j, \lambda_n) = -\frac{1}{4\pi} \frac{\kappa_i \ln\lambda_n - \kappa_i \ln\kappa_i + \kappa_i - \lambda_n}{\kappa_i(\kappa_i - \lambda_n)^2} \tag{C.22}$$

and for $\lambda_n = \kappa_i = \kappa_j$ and $\Lambda \gg \lambda_n$

$$I_3(V, a, \kappa_i = \kappa_j = \lambda_n) = -\frac{1}{8\pi\kappa_i^2} \tag{C.23}$$

Bibliography

[1] Roman Orus, *A Practical Introduction to Tensor Networks:Matrix Product States and Projected Entangled Pair States*, Institute of Physics, Johannes Gutenberg University (2014).

[2] Roman Orus, *Tensor networks for complex quantum systems*, Nature Reviews Physics volume **1**, pages 538–550 (2019).

[3] F. Verstraete, J.I. Cirac, V. Murg, *Matrix product states, projected entangled pair states, and variational renormalization group methods for quantum spin systems*, Adv. Phys.**57**, 143(2008).

[4] J. I. Cirac and F. Verstraete, *Renormalization and Tensor Product States in Spin Chains and Lattices*,J. Phys. **A42**,504004 (2009).

[5] J. C. Bridgeman and C. T. Chubb, *Hand-Waving and Interpretive Dance: An Introductory Course on Tensor Networks*, J. Phys. **A50**, 223001 (2017).

[6] *Time-evolution methods for matrix-product states*,S. Paeckela, T. Köhler, A. Swobodac, S. R. Manmanaa, U. Schollwöckc ,C. Hubig, https://arxiv.org/pdf/1901.05824.pdf

[7] Piotr Czarnik and Jacek Dziarmaga, *Time evolution of an infinite projected entangled pair state: An algorithm from first principles*, Phys. Rev. B **98**, 045110 (2018)

[8] F. Pollmann, A. M. Turner, E. Berg, and M. Oshikawa, *Entanglement Spectrum of a Topological Phase in One Dimension*, Phys. Rev. **B81**, 064439 (2010).

[9] N. Schuch, D. Perez-García, and .I Cirac, *Classifying Quantum Phases Using Matrix Product States and Projected Entangled Pair States*,Phys. Rev. **B84**, 165139(2011).

[10] H. A. Kramers , G. H. Wannier, *Statistics of the two-dimensional ferromagnet*, Part II. Phys. Rev.60, 263 (1941).

[11] S. R. White, *Density matrix formulation for quantum renormalization groups*. Phys. Rev. Lett.**69**, 28632866 (1992).

[12] U. Schollwöck, *The density Matrix Renormalization Group*, Rev. Mod. Phys. **77**, 259 (2005)

[13] F. Verstraete, J. I. Cirac, *Renormalization algorithms for quantum- many body systems in two and higher dimensions*. Preprint at https://arxiv.org/abs/cond-mat/0407066 (2004).

[14] G. Vidal, *Entanglement renormalization*, Phys. Rev. Lett.**99**, 220405 (2007).

[15] B. Swingle, *Entanglement renormalization and holography*, Phys. Rev. **D86**, 065007 (2012).

[16] M. M. Wolf, F. Verstraete, M. B. Hastings, and J. I. Cirac, *Area Laws in Quantum Systems: Mutual Information andCorrelations*, Phys. Rev. Lett.**100**, 070502 (2008)

[17] M. B. Hastings, *Solving gapped Hamiltonians locally*. Phys. Rev. **B73**, 085115 (2006).

[18] F. Verstraete, J.I. Cirac, *Continuous Matrix Product States for quantum Fields*, Phys. Rev. Lett. **104**, 190405 (2010).

[19] J. Haegeman, J. I. Cirac, T. J. Osborne, and F. Verstraete, *Calculus of Continuous Matrix Product States*,Phys. Rev. **B88**, 085118 (2013).

[20] J. Haegeman, T. J. Osborne, H. Verschelde, F. Verstraete, *Entanglement renormalization for quantum fields in real space*, Phys. Rev. Lett.**110**, 100402 (2013).

[21] C. Brockt, J. Haegeman, D. Jennings, T.J. Osborne F. Verstraete, *The continuum limit of a tensor network: a path integral representation.*, arXiv:1210.5401

[22] Antoine Tilloy, J. Ignacio Cirac, *Continuous Tensor Network States for Quantum Fields*, Phys.Rev.X **9**,021040 (2019).

[23] D. Jennings, C. Brockt, J. Haegeman, T.J. Osborne, and F. Verstraete, *Continuum Tensor Network Field States, Path Integral Representations and Spatial Symmetries*,New J.Phys.**17**, 063039 (2015).

[24] Riccardo Borghi, *The variational method in quantum mechanics: An elementary introduction*, Eur. J. Phys.**39** 035410 (2018)

[25] J. Haegeman, J. I. Cirac, T. J. Osborne, H. Verschelde, and F. Verstraete, *Applying the Variational Principle to (11)-Dimensional Quantum Field Theories*, Phys. Rev. Lett. **105**,251601 (2010)

[26] G. Vidal, *Efficient classical simulation of slightly entangled quantum computations*. Phys. Rev. Lett.**91**, 147902 (2003).

[27] M.B. Hastings, *An Area Law for One Dimensional Quantum Systems*, J.Stat.Mech., P08024 (2007).

[28] E. H. Lieb and W. Liniger, Phys. Rev. 130, 1605 (1963)

[29] V. Stojevic, J. Haegeman, I. P. McCulloch, L. Tagliacozzo, F. Verstraete, *Conformal Data from Finite Entanglement Scaling*, arXiv:1401.7654

[30] J. Jordan,R. Orús,G. Vidal, F. Verstraete, J. I. Cirac, *Classical simulation of infinite-size quantum lattice systems in two spatial dimensions*. Phys. Rev. Lett.**101**, 250602 (2008).

[31] R. Orús, G. Vidal, *Simulation of two- dimensional quantum systems on an infinite lattice revisited: corner transfer matrix for tensor contraction*. Phys. Rev. **B80**, 094403 (2009).

[32] M. Levin, C. P. Nave, *Tensor renormalization group approach to two- dimensional classical lattice models*, Phys. Rev. Lett.**99**, 120601 (2007)

[33] T. Guaita, L. Hackl, T. Shi, C. Hubig, E. Demler, J. Ignacio Cirac *Gaussian time dependent variational principle for the Bose-Hubbard model*, Phys. Rev. B **100**, 094529 (2019)